JOURNAL OF CATALYSIS **158,** 452–476 (1996)
ARTICLE NO. 0046

Catalytic Synergy in the Oxidative Dehydrogenation of Propane over MgVO Catalysts

S. R. G. Carrazán,[1] C. Peres, J. P. Bernard, M. Ruwet, P. Ruiz, and B. Delmon

Unité de Catalyse et Chimie des Matériaux Divisés, Université Catholique de Louvain, Place Croix du Sud 2 boite 17, 1348 Louvain-la-Neuve, Belgium

Received December 27, 1994; revised September 8, 1995; accepted September 11, 1995

Synergetic effects in the oxidative dehydrogenation of propane have been studied over magnesium vanadate catalysts containing three different Mg/V ratios: 1/2, 2/2, and 3/2, denoted as MgV(1/2), MgV(2/2), and MgV(3/2). Four types of catalysts were analysed: (a) pure magnesium vanadate oxides, (b) mechanical mixtures of the pure magnesium vanadate oxides, (c) mechanical mixtures of the magnesium vanadate oxides with α-Sb_2O_4, and (d) impregnated MgV(2/2) and MgV(3/2) with Sb ions. Synergetic effects are observed in MgV(3/2) and in MgV(2/2) oxides when they are in presence of α-Sb_2O_4. In the mixtures of MgV(3/2) with α-Sb_2O_4, the principal effect is an increase in the selectivity with a corresponding decrease in propane conversion, whereas in the mixtures of MgV(2/2) with α-Sb_2O_4, there is a strong increase in propane conversion with a moderate increase in propene yield. Concerning the mixtures of MgV(3/2) and MgV(2/2), synergetic effects in the conversion, in the yield, and in the selectivity are observed. However, no synergetic effects in selectivity or conversion are exhibited by MgV(2/2) and MgV(3/2) when they are mixed with MgV(1/2). Highly dispersed (Sb_xO_y), formed on impregnated MgV(2/2) and MgV(3/2), sinters and detaches from MgV(2/2) and MgV(3/2) surfaces. No formation of a new phase or contamination in the presence of α-Sb_2O_4 takes place when MgV(3/2) is used. Thus, these catalysts contain two separate phases in contact. In MgV(2/2) + α-Sb_2O_4 mechanical mixtures a new phase, $MgSb_2O_6$, (formed during the test) is also present in small quantities. The mixtures of MgV(3/2) with MgV(2/2) reveal neither formation of a new phase nor contamination. The synergetic effects in the selectivity exhibited by MgV(3/2) mixed with MgV(2/2) and with α-Sb_2O_4 is explained by a remote control mechanism. $MgSb_2O_6$, formed in MgV(2/2)-containing catalysts, is responsible for the increase in complete oxidation and the strong decrease in selectivity.

1. INTRODUCTION

Catalysts containing magnesium, vanadium, and oxygen (MgVO) are presently under intensive study. They are promising for the industrially important oxidative catalytic dehydrogenation (OD) of alkanes. These catalysts seem to provide adequate quantities of the oxygen species to activate the reaction of alkanes into alkenes (and dienes) at relatively low temperatures, thus avoiding total oxidation (1–3).

Three different crystalline phases, namely, β-MgV_2O_6 (methavanadate), α-$Mg_2V_2O_7$ (pyrovanadate), and $Mg_3V_2O_8$ (orthovanadate), have been observed in MgVO catalysts. For simplicity, they are referred to as MgV(1/2), MgV(2/2), and MgV(3/2) phases, respectively. Different explanations of their activity have been given.

Chaar *et al.* (1, 2) prepared different MgVO catalysts by impregnation of MgO powder with basic aqueous solutions of ammonium vanadate. Only the presence of MgV(3/2) phase has been detected in these catalysts. The authors found that they were selective for the OD of alkanes to alkenes. The absence of any oxygenate products was attributed to the fact that alkenes adsorb relatively weakly on MgVO catalysts and the MgVO surface does not contain a high concentration of oxygen active for oxidation. The weak adsorption of basic alkene molecules on those catalysts is explained by the fact that MgVO catalysts are also basic. Concerning the surface active oxygen, they consider that V=O groups are very important for oxygenate formation. They support such an explanation on the basis of previous results (3–5) in which it was shown that the activity of the V_2O_5, either unsupported or supported on TiO_2 and Al_2O_3, could be correlated with the amount of surface V=O species. These V=O groups possess a characteristic infrared stretching frequency around 1022 cm^{-1} which is also present on V–P–O catalysts (6). However the presence of that band is not observed on the MgV(3/2) phase. Consequently, they argue that if this V=O group is important for oxygenate formation, the fact that oxygen is not in the form V=O on the MgV(3/2) phase may account for the absence of oxygenate formation.

However, Siew Hem Sam *et al.* (7) have observed, in catalysts prepared by impregnating $Mg(OH)_2$ with vana-

[1] On leave from Departamento de Química Inorgánica, Facultad de Química, Universidad de Salamanca, España.

0021-9517/96 $12.00

date solutions and subsequent calcination at different temperatures, that the maximum yield and selectivity for the OD of propane were obtained in cases where the MgV(2/2) phase had developed. When testing the single phases, they found that the MgV(2/2) phase was both more active and selective for the OD of propane, producing minor amounts of oxygenates, principally acrylaldehyde. Conversely MgV(3/2) would be responsible for total oxidation and MgV(1/2) would not be very selective for the OD of propane and leads principally to ethanal. The specificity of the MgV(2/2) phase is explained by considering the difference in the local environment of vanadium by oxygen atoms in the three different vanadates. In the MgV(3/2) phase, vanadium ions are in isolated tetrahedral sites. In MgV(2/2), V_2O_7 units are formed by two corner-sharing VO_4 distorted tetrahedra with long V–O bridges within these groups. A short V–O bond is also observed in one of the tetrahedron. In MgV(1/2), vanadium ions are in highly distorted octahedral sites. The authors argue that the presence of two different V–O bonds in the MgV(2/2) phase is responsible for the specificity of this phase for the selective OD of propane. The V–O short bond could initiate a hydrogen abstraction and the bridging O could participate in the OD mechanism by catalyzing the formation of water.

The highest selectivity for the OD of propane was also attributed to the MgV(2/2) phase by Guerrero Ruiz *et al.* (8). The stabilization of V^{4+} ions associated with surface oxygen vacancies and the easy reducibility of the MgV(2/2) phase seem to favor the oxygen atom extraction from this phase compared to the MgV(3/2) phase.

An attempt to explain the selectivity of the reaction of oxygen with different alkanes over three catalysts, MgV(2/2), MgV(3/2), and phosphorous vanadium VPO (containing principally $(VO)_2P_2O_7$) phase), has been presented by Michalakos *et al.* (9). In propane oxidation, they found only CO as the predominant product on the VPO catalysts whereas propene was detected with MgV(2/2) and MgV(3/2) catalysts.

The authors make an attempt to explain the catalytic activity and selectivity pattern observed in these catalysts by considering both the nature of the active site and the size of the surface intermediate (in this case a propyl radical). In the case of the $(VO)_2P_2O_7$ phase, the V_2O_8 structural units (active sites) would contain the reactive lattice oxygen which is supposed to be an oxygen ion bridging two easily reducible vanadium ions. It is possible to calculate the appropriate size of the propyl radical which would allow it to bond to both vanadium ions constituting the active site (the separation of the vanadium ions in the catalysts being estimated from crystallographic data) and thus to be readily attacked by the reactive lattice oxygen. Thus, the formation of fully oxidized products would then be the favored reaction. Otherwise, dehydrogenation should be the predominant reaction. Considering this, the authors argue that propane would react on MgV(2/2) as if the reactive sites were isolated VO_4 units, as in MgV(3/2), in which there is no oxygen ion bridging two vanadium ions. This explanation would imply that the oxygen ions in MgV(3/2) have a lower tendency to form C–O bonds. The formation of propene on both MgV(2/2) and MgV(3/2) is explained by using this assumption.

In a recent paper, Wang *et al.* (10) compared the catalytic and electrocatalytic oxidations of propane on MgVO catalysts prepared in a way similar to that reported by Chaar *et al.* (2). Their results appear to indicate that electrochemical supplied oxygen is more selective toward propene than oxygen supplied from the gas phase. The reactor used was an yttrium–zirconium tube inside which the catalyst was deposited; the outside bottom of the tube was painted with two patches of Ag film which acted respectively as counter and reference electrodes. This assembly was connected to a variable resistance and to a galvanostat/potentiostat (GP). Thus, depending on the on/off switch of the GP, oxygen could be pumped toward or from the catalyst by the externally applied current. Mechanisms of both catalytic and electrocatalytic oxidation of propane were tentatively suggested. Surface oxygen vacancy in the neighborhood of a surface vanadium ion was identified as surface active species. This oxygen ion vacancy could be filled either from oxygen in the gas feed or electrically supplied oxygen. The rate determining step would involve heterolytic splitting of a methylenic CH bond in the C_3H_8 molecule to form a surface bonded C_3H_7-ion and a surface hydroxyl ion. The subsequent extraction of a methyl hydrogen by the formed surface hydroxyl ion in the neighborhood would lead to the desorption of H_2O and C_3H_6.

On the other hand, Gao *et al.* (11) confirmed the dependence between the activity of MgVO catalysts and the Mg/V ratio suggested by Chaar *et al.* (1, 2) and Siew Hew Sam *et al.* (7).

In a recent work (12) a new phenomenon has been observed. The catalytic performances of a two-phase MgVO catalyst are very different from those of the corresponding pure phases; namely, the selectivity of the MgV(3/2) phase can be improved by the MgV(2/2) phase when there is an excess of magnesium with respect to the stoichiometry of this second phase. This suggests that the presence of more than one phase can promote the selectivity in the reactions of propane with oxygen.

In the present work, an attempt is made to identify the factors operating in this kind of promoter effect, as observed in multiphase catalysts during the oxidative dehydrogenation of propane. A starting hypothesis can be that phase cooperation could be due to remote control (13–22), a mechanism which has been shown to operate on the oxidation of olefins to unsaturated aldehydes (13, 14, 16), the oxidative dehydrogenation of ethanol to acetaldehyde

(17), the oxidative dehydrogenation of butene to butadiene (18), the oxidation of butane to maleic anhydride (19, 20), and the dehydration of *N*-ethyl formamide to propionitrile (an oxygen-aided reaction) (10). As α-Sb_2O_4, as an external phase, was shown to promote selectivity of the active phases in these four reactions, we studied mixtures of catalysts which contained principally MgV(1/2), MgV(2/2), and MgV(3/2) catalysts on the one hand and α-Sb_2O_4 on the other.

The strategy followed in this work was to prepare separately powders containing one of the three phases, to mix them with α-Sb_2O_4, and to study the synergetic effects. Aside from the remote control, a common explanation of synergy in such experiments is the formation of a surface contamination layer of elements of one phase on the surface of the other phase. In order to examine a possible tendency of mutual contamination between MgVO catalysts and antimony, samples of MgVO catalysts artificially contaminated with Sb, namely impregnated with Sb ions, were also prepared.

Another explanation of the synergetic effects is the formation of a new phase. The influence of such a new phase associating two (Mg, Sb) elements in a mixed compound has also been studied by preparing mixed phases, in particular $MgSb_2O_6$, and studying their catalytic activity.

Some thermal pretreatments, of long duration, involving mixtures of MgVO + α-Sb_2O_4 have also been carried out. The objective of these treatments was to further investigate a possible tendency of the oxides in the mechanical mixtures to react together and to form new phases.

In general, MgVO catalysts are not constituted of pure isolated phases. As discussed above, it is therefore interesting to also study the synergetic effects existing between two different MgVO catalysts. For this reason catalyst mixtures of MgV(2/2) + MgV(3/2), MgV(2/2) + MgV(1/2), and MgV(3/2) + MgV(1/2) have also been investigated.

In order to correlate the catalytic activity with the solid-state characteristics of the single and the biphasic catalysts, a detailed physicochemical characterization was carried out on all catalysts before and after the catalytic test or after the thermal pretreatments.

X-ray diffraction measurements were performed to determine the crystalline phases and also to detect phase modifications or formation of new compounds.

Surface contamination was studied by means of analysis by electron microscopy (AEM) and photoelectron spectroscopy (XPS). AEM can yield information concerning the composition of each particle of each phase and XPS can reveal the composition of the outermost surface layers of the samples and detect the transformations occurring at 15–20 monolayers of depth from the external surface.

As surface oxygen plays a role in the reaction, and several interpretations take into account the ease with which oxygen from the surface can react with the hydrocarbon, thermoreduction measurements were also carried out. Acidity has often been mentioned as an important property for oxidation catalysts. For this reason acidity was measured by ammonia TPD (NH_3 TPD).

One of the teachings of this paper is that the catalytic activity of the MgVO system is not easy to reproduce with high precision. The results presented in this paper correspond to research executed in this laboratory over a long period of time and by many researchers. In spite of the precautions taken during the experiments, some dispersion in the results has been observed. The reasons for that dispersion are not clear. It is hoped that this work would help to understand and to control such irreproducibility.

2. EXPERIMENTAL

2.1. Materials

The products used as starting materials for catalyst preparation were: ammonium metavanadate (NH_4VO_3), antimony (III) oxide (Sb_2O_3), and antimony (III) acetate ($Sb(C_2O_2H_3)_3$ all from Merck (p.a. grade); magnesium hydroxide ($Mg(OH)_2$) (Merck, purity 95%), magnesium nitrate ($Mg(NO_3)_2 \cdot 6H_2O$) (Fluka, p.a. grade), and citric acid ($C_6O_7H_8$) from UCB (p.a.). HCl was Janssen p.a., 37%. Gases were from L'Air Liquide, propane > 99%, He 99.995%, H_2 99.99997%, NH_3 99.998%, and O_2 99.5%; they were used without any further purification.

2.2. Catalyst Preparation

2.2.1. Single-Phase Catalysts

Three types of oxides were prepared.

(*a*) *Antimony oxide*. Pure α-Sb_2O_4 was obtained by calcination of Sb_2O_3 in air at 873 K for 20 h.

(*b*) *Magnesium vanadate oxides*. Pure MgVO oxides with Mg/V atomic ratios = 1/2, 2/2, and 3/2 were prepared by the citrate method (23) which is known to be a powerful method for making homogeneous oxides containing two or several metallic elements.

The main preparation steps of the MgVO catalysts according to the citrate method were as follows. First, a transparent solution of magnesium nitrate or magnesium hydroxide and ammonium metavanadate with the desired atomic Mg/V ratio were prepared. Then citric acid was added in such a proportion to have 1.1 equivalent-gram of acid function per valence-gram of metal. The solution thus obtained was evaporated in a Rotavapor at 308 K until a viscous solution was obtained. The viscous solution was dried at 353 K for 15 h (an amorphous solid organic compound was obtained). This compound was decomposed at 573 K for 16 h. Finally the calcined solid was ground into a fine powder. The amounts of reagents, tem-

TABLE 1

MgV(*X*) Preparation Conditions

Sample	NH_4VO_3 (g)	$Mg(HO)_2$ (g)	$Mg(NO_3)_2 \cdot 2H_2O$ (g)	Citric Acid (g)	Temperature (K)	Time (h)
MgV(1/2)0	21.1	5.3		58	773	10
					823	6
					873	6
					923	6
MgV(2/2)0	17.8	8.9		65	773	10
					823	6
					873	6
					923	6
MgV(2/2)I	8.9		19.5	41.1	833	20
MgV(2/2)II	8.9		19.5	41.1	873	15
MgV(2/2)III	8.9		19.5	41.1	873	15
MgV(2/2)IV	8.9		19.5	41.1	873	15
MgV(3/2)0	15.4	8.9		6.5	773	10
					823	6
					873	6
					923	6
					973	6
MgV(3/2)I	7.7		25.4	40.7	873	20
MgV(3/2)II	7.7		25.4	40.7	873	15
					973	7
					1073	20
MgV(3/2)III	7.7		25.4	40.7	873	20
MgV(3/2)IV	7.7		25.4	40.7	923	20

Note. 0, I, II, III, and IV indicate preparation number.

perature, and time of calcination to obtain 10 g (I, II, III, and IV) or 20 g (0) of these catalysts are reported in Table 1 (numbers denote MgVO preparation conditions) and the nomenclature in Table 2.

(*c*) *Magnesium antimonate*. Pure $MgSb_2O_6$ was prepared in a similar procedure as indicated for the preparation of magnesium vanadate catalysts but in this case, antimony acetate in an aqueous HCl solution and magnesium nitrate were used. Temperature and time of calcination were 873 K and 20 h, respectively.

2.2.2. Two-Phase Catalysts

These catalysts were prepared from MgV (1/2), MgV(2/2), Mg/V (3/2), and α-Sb_2O_4, either by mechanically mixing or by impregnation of the MgV catalysts with Sb ions. Pure MgVO oxides were submitted to a similar treatment to that used to prepare the two-phase catalysts.

(*a*) *Mechanical mixtures of MgV(2/2) + MgV(1/2), MgV(3/2) + MgV(1/2), and MgV(3/2) + MgV(2/2).* These were prepared by dispersing both oxides in *n*-pentane by magnetically stirring for 30 min. The suspension was then stirred in an ultrasonic vibrator Transonic 32 for 10 min at room temperature. After evaporation of the *n*-pentane under reduced pressure and continuous agitation, the mixtures so obtained were finally dried in air at 353 K overnight. These mixtures will be denoted in the following manner (see Table 2): MMgV(*X*)0MgV(*Y*) or MMgV(*X*)IIMgV(*Y*), in which *X* (or *Y*) is the Mg/V atomic ratio and 0 or II denote MgV(*X*) preparation conditions (Table 1).

(*b*) *Mechanical mixtures of MgV(2/2) or MgV(3/2) oxides with α-Sb_2O_4.* Two methods were employed for the preparation of these mixtures:

(i) Intensive agitation: This involved vigorously mixing the suspension of the powders in 200 ml of a light paraffin (*n*-pentane) for 3 min by means of a mixer (Ultra-Turrax from Janke & Kunkel) at room temperature. After evaporation of the *n*-pentane under reduced pressure, the mixtures so obtained were finally dried in air at 323 K overnight. They will be denoted as in the following MMgV(*X*)ISb(ia) (see Table 2). Symbols as in 2.2.2.a.

(ii) Magnetic agitation: The same method was used as for the preparation of the MMgV(*X*)ISb(ia), except that the suspension was only agitated magnetically for 20 min. No Ultra-Turrax mixer was used. Samples will be denoted as in the following MMgV(*X*)0Sb or MMgV(*X*)ISb (see Table 2). Symbols as in 2.2.2.a.

(*c*) *Expression of the mechanical mixture composition.*

TABLE 2

Preparation Conditions and Notation for the Single and Multiphasic Catalysts

Catalyst	Preparation method	V/Mg	Preparation number (n)	Notation
Single Phase	Citric method	1/2, 2/2, 3/2	0, I, II, III, IV	MgV(1/2)n, MgV(2/2)n, MgV(3/2)n
Two phases	Mechanical mixtures of single phase oxides by magnetic stirring	Between single phase MgV(X) (X = 1/2, 2/2, 3/2) catalysts		MMgV(2/2)0MgV(1/2) MMgV(2/2)0MgV(1/2) MMgV(2/2)0MgV(2/2) MMgV(2/2)IIMgV(1/2) MMgV(2/2)IIMgV(1/2) MMgV(3/2)IIMgV(2/2)
		Between MgV(X) (X = 1/2, 2/2, 3/2) and α-Sb_2O4		MMgV(2/2)0Sb MMgV(3/2)0Sb MMgV(2/2)ISb MMgV(3/2)ISb
	Mechanical mixtures of single phase oxides by intensive agitation	Between MgV(X) (X = 1/2, 2/2, 3/2) and α-Sb_2O4		MMgV(2/2)IS(ia) MMgV(3/2)ISb(ia)
	Impregnation	MgV(X) (X = 2/2, 3/2) with Sb ions		MgV(2/2)III/L MgV(3/2)III/L
	Calcination of mechanical mixtures			MMgV(2/2)IVSb/T MMgV(3/2)IVSb/T

The composition is expressed as mass ratio by Rm = weight A/(weight A + weight B), where A is one of the MgVO oxides and B is α-Sb_2O_4, for the mixtures with α-Sb_2O_4 (see Section 2.2.2.b) or the other MgVO oxide, for the mixtures between the two MgVO oxides (see Section 2.2.2.a). In the case of MMgV(X)0Sb and MMgV(X)0MgV(Y) mechanical mixtures the Rm values are 0, 0.5, and 1.0 and for MMgV(X)ISb(ia) and MMgV(X)IIMgV(Y) mechanical mixtures the Rm values are 0, 0.25, 0.5, 0.75, and 1.

(*d*) *MgV(2/2)III and MgV(3/2)III catalysts impregnated with antimony ions.* Nominal loadings corresponding to the weight of α-Sb_2O_4 theoretically necessary to form one or three monolayers (''nominal'' loadings) were prepared by impregnation. The preparation method is similar to that reported by Weng *et al.* (13). The quantity of antimony necessary to form one monolayer of α-Sb_2O_4 on the surface of the MgV(2/2)III and MgV(3/2)III was calculated on the basis of the BET surface area and the dimension of the unit cell of α-Sb_2O_4. This value is 0.16 nm^2, assuming that α-Sb_2O_4 is deposited according to the arrangement of the (100) face and that the α-Sb_2O_4 layer has the thickness of the unit cell. Values of 1.46 and 3.18% were calculated for the percentage in weight of α-Sb_2O_4 necessary to form one monolayer on the surface of the MgV(2/2)III (3.3 m^2/g) and on the MgV(3/2)III(7.2 m^2/g) samples, respectively.

The procedure followed for the preparation was as follows: 250 ml of a $CHCl_3$ solution containing Sb^{3+} and Sb^{5+} ions with a ratio Sb^{3+}/Sb^{5+} = 1 was prepared with 7.40 g of $SbCl_3$ and 9.65 g of $SbCl_5$. The quantities of the Sb^{3+}/Sb^{5+} solution required to form 1 or 3 monolayers on the surface of 1.5 g of MgV(2/2) III or MgV(3/2)III (0.5 or 1.5 ml for MgV(2/2)III and 1.3 or 3.9 ml for MgV(3/2)III) were dissolved in 75 ml of $CHCl_3$. Slow evaporation of the solvent was performed in the Rotavapor at 308 K under reduced pressure. The powder thus obtained was washed with a very dilute NH_3 solution in order to eliminate Cl^- (complete elimination was checked with $AgNO_3$ solution). The powder was finally dried at 383 K overnight. The catalysts were used as such, without calcination.

The same procedure was also used for the pure MgV(2/2)III and MgV(3/2)III catalysts. Samples were denoted (see Table 2) as MgV(X)III/L, in which X is the Mg/V atomic ratio of the catalysts and L is the number of monolayers deposited on the catalyst (1 or 3).

(*e*) *Calcined mechanical mixtures of MgV(2/2)IV + α-Sb_2O_4 or MgV(3/2)IV + α-Sb_2O_4.* Two mechanical mixtures, MgV(2/2)IV with α-Sb_2O_4 and MgV(3/2)IV with α-Sb_2O_4, each with Rm = 0.5, were both calcined using two different conditions: (i) 823 K for 1, 3, and 6 days and (ii) 923 K for 2 days. Samples were denoted (see Table 2) as MMgV(X)IVSb/T, T being the temperature of calcination in K.

(*f*) *Mechanical mixture of $MgSb_2O_6$ + α-Sb_2O_4 (Rm =*

0.5). This was prepared by the procedure described in 2.2.2.b (ii).

2.3. Catalyst Characterization

All catalysts were characterized before and after the catalytic test using the following physicochemical methods.

2.3.1. BET Surface Areas

BET surface areas were measured using a Micromeritics ASAP 2000 instrument by adsorption of krypton at 77 K on 200 mg of samples previously degassed at 423 K for 2 h. Theoretical specific surface areas for the fresh mechanical mixtures of catalysts A and B were calculated by the equation

$$(S_{BET})_{theo} = (S_{BET})_A \cdot Rm + (S_{BET})_B \cdot (1 - Rm),$$

in which $(S_{BET})_A$ and $(S_{BET})_B$ are the BET surface areas of the oxides A and B, respectively, and Rm is the mass ratio is defined as in 2.2.2.c.

2.3.2. X-Ray Diffraction (XRD)

XRD patterns were obtained with a KRISTALLOFLEX Siemens D5000 diffractometer using Cu$K\alpha$1 radiation (λ = 154.18 pm) and a secondary monochromator. A Ni filter was used. The samples, in powder form, were analyzed without treatment after deposition on a quartz monocrystal sample holder supplied by Siemens. The identification of crystalline phases was made using references from the literature and the ASTM files (DIFRACT-AT software/SOCABIM). The percentage purity of a phase was estimated from the ratio of the integrated areas of the most relevant peaks of the phase and the impurity (2Θ = 35.22 for MgV(3/2) and 2Θ = 28.03 for MgV(2/2)).

2.3.3. X-Ray Photoelectron Spectroscopy

XPS analyses were performed with an SSX-100 model 206 X-ray photoelectron spectrometer from FISONS. The analysis chamber was operated under ultrahigh vacuum with a pressure close to 5×10^{-9} Torr. X-rays produced by a monochromatized aluminum anode (Al$K\alpha$ = 1486.6 eV) were focused in an area of around 1 mm^2 (1000 μm spot). The pass energy was set at 50 eV (resolution 2); under these conditions the energy resolution (FWHM, full width at half maximum, of Au $4f_{7/2}$) was 1.0 eV. The surface positive charge originating from the ejection of photoelectrons was compensated by a ''floodgun'' operating at 6 eV using a nickel grid set at 3 mm above the samples. Powdered samples were placed into small troughs.

The C 1*s*, V $2p_{3/2}$, V $2p_{1/2}$, O 1*s*, Sb $3d_{3/2}$, Mg 2*s*, and C 1*s* bands were swept successively. The Sb $3d_{5/2}$ peak overlaps the O 1*s* peak. In some catalysts, the most intense Mg (Auger) peak was swept instead of Mg 2*s*. The binding energy (BE) values were calculated with respect to C 1*s* (BE of C–C,H fixed at 284.8 eV).

The composite peaks (like O 1d*s*–Sb 3*d* band and V 2*p* peaks) were decomposed by the least squares fitting routine provided by the spectrometer manufacturer.

In the decomposition process the Gaussian/Lorentzian ratio was 85/15, the difference in binding energies between the V $2p_{3/2}$ and V $2p_{1/2}$ peaks was set to 7.3 eV, and the V $2p_{3/2}$/V $2p_{1/2}$ ratio was set to 2.0. The decomposition of the V 2*p* peaks with no area and interval constraints was also carried out.

Nonpretreated V_2O_5 and V_2O_4 standards have been analyzed. Also V_2O_5 standard pretreated in O_2 atmosphere and calcined simultaneously for 13 h at 773 K, as well as V_2O_4 standard pretreated in H_2 atmosphere and calcined simultaneously at 393 K for 1 h, have been analyzed. Particular precautions have been taken with the pretreated samples: in order to avoid contact with the atmosphere the powder was kept and pressed in *n*-octane. The powder covered with an *n*-octane droplet was immediately pumped in the preparation chamber.

The XPS atomic ratios V/Mg, V/Sb, Sb/Mg, C/Mg, C/V, and C/Sb were calculated from XPS intensities by using atomic sensitivity factors provided by the spectrometer manufacturer.

The theoretical V/Mg ratio was calculated from the sample stoichiometry whereas the V/Sb ratio was estimated by the expression

$$\text{V/Sb theo} = \frac{Rm/Mw[\text{MgV(3/2) or MgV(2/2)}]}{1 - Rm/Mw[\alpha\text{-}Sb_2O_4]},$$

where Mw is the molecular weight.

2.3.4. Electron Microscopy and Electron Microanalysis

Transmission electron microscopy (TEM) and electron microanalysis (AEM) were performed with a JEOL-JEM 100 C TEMSCAN equipped with a Kevex 5100 C energy dispersive spectrometer for electron probe microanalysis (EPMA). The accelerating potential was 100 kV. The samples were ground, dispersed in *n*-pentane with an ultrasonic vibrator, and deposited on a thin carbon film supported on a standard copper grid.

In principle, AEM permits the detection of a contaminant at the level of 1%.

2.3.5. Vanadium Oxidation State

The average oxidation state of vanadium was determined by double titration. The main titration steps were as follows: 200 mg of catalyst were dissolved in 200 ml of hot H_2SO_4 (2 *M*) solution. The obtained solution was first titrated with 0.02 *M* $KMnO_4$ (volume 1) which oxidizes

the V^{3+} and V^{4+} ions into V^{5+}. This was followed by adding an excess of 1 *N* $Fe(NH_4)_2(SO_4)_2$ acidified with 2 *M* H_2SO_4 to reduce the V^{5+} ions into V^{4+}. The solution thus obtained was cooled and then 20 mg $(NH_4)_2S_2O_8$ were added to oxidize the excess Fe^{2+} ions. Finally the V^{4+} ions were titrated with 0.02 *M* $KMnO_4$ (volume 2). The average oxidation state of vanadium was calculated by oxidation state = 5 − (volume 1/volume 2).

2.4. Temperature Programmed Desorption of NH_3 (NH_3 TPD)

TPD was carried out using a versatile apparatus equipped with a thermal conductivity detector (24, 25). Samples MMgV(*X*)0Sb with *Rm* = 0.5 were studied. As α-Sb_2O_4 does not show any adsorption of NH_3, experiments were carried out with the same amount of the MgV(*X*)0 components in the catalyst, namely 200 mg of pure MgV(*X*)0 catalysts and 400 mg for the mixture. Samples were pretreated under helium at 723 K for 30 min. After cooling at 298 K they were exposed to NH_3 for 30 min and flushed, at that temperature, with helium for 30 min. NH_3 TPD measurements were carried out from room temperature to 723 K under a flow of helium and at a heating rate of 10 K/min.

Weak, intermediate, and strong acidity have been arbitrary ascribed to the acid sites describing NH_3 three ranges of temperatures: weak acidity from 373 to 473 K, intermediate acidity from 473 to 573 K, and strong acidity above 573 K.

The acidity distribution of catalysts has been expressed as the ratio between the integrated area of the NH_3 band developed in a given range of temperature and the total integrated area of the NH_3 band. A total specific acidity is calculated by dividing the total area of the NH_3 band by the BET surface area of the sample.

2.5. Thermoreduction and Thermo-oxidation Measurements

Thermoreduction experiments (TR) were carried out with a Setaram MTB 10-8 microbalance connected to a vacuum and gas-handling system. The catalyst (30 mg) was outgassed under vacuum (10–3 Torr "1Torr = 133.3 N m^{-2}") at 723 K for 15 min; H_2 was introduced at a partial pressure of 760 Torr. The reduction was carried out at 723 K for 2 h. The sample weight changes due to reduction were recorded as a function of time. Once reduction was complete, a vacuum was employed (10–3 Torr) and oxygen was introduced (partial pressure of 760 Torr). The sample weight changes were recorded again as a function of time.

The relative weight change percentage is defined as the ratio between loss of sample weight (Δm) and sample initial weight (m_o).

2.6. Catalytic Activity Measurements

2.6.1. Reaction Test

The catalytic tests were carried out in a continuous gas-flow system. The catalyst (particle size between 500–800 μm) was supported on a fixed quartz chip bed (density N4, thickness about 2 mm) in a U-type quartz microreactor (internal diameter 24 mm) operating under atmospheric pressure. The reactor was inserted in an electrically heated furnace. The temperature of the catalyst bed was monitored by a thermocouple placed in a thermowall in the center of the bed. The composition and the flow rate of the gas feed mixture were measured using mass flow controllers which were calibrated for each specific gas (propane, oxygen, and helium).

Before reaching the reactor, the gas feed mixture passed through a preheater at 503 K. Electronic devices controlled by thermocouples inserted in the furnace and preheater were used. The lines between the reactor and the chromatograph were kept at 423 K to prevent any condensation of the reaction products.

The reaction conditions were as follows: (i) for catalysts containing MgV(*X*)0, partial pressures for propane, oxygen, and helium were 60.8, 182.4, and 516.8 Torr, respectively; the total feed was 37 ml/min and the reaction temperature was 823 K. The amounts of catalyst were 70, 100, and 200 mg. The volumes of the catalyst bed were 0.27, 0.39, and 0.77 cm^3 and contact times were 0.44, 0.63, and 1.26 s. (ii) for all the other tests, partial pressures of propane, oxygen, and helium were 42.4, 114.6, and 603 Torr, respectively; the total feed was 33 ml/min and the reaction temperatures were 773, 793, and 813 K. In the case of samples containing MgV(*X*)I catalyst (noncalcined and calcined), 500 mg were used for the of impregnated samples. For those containing MgV(*X*)II catalysts, 1g was used. For samples containing $MgSb_2O_6$, 200 mg were used. The volumes of catalyst bed were 0.8, 0.9, and 3.4 cm^3 and the contact times were 1.45, 1.63, and 6.18 s, respectively. The range of rates of reaction per unit area are calculated from the lowest and the highest conversion values for each type of catalyst.

Under the conditions used for samples containing MgV(*X*)0 catalysts, the empty reactor showed a small activity (less than 2% conversion and less than 1% propene yield, which represents above 10% of the propane conversion and the propene yield measured during experiments). No activity was observed for the empty reactor. Tests using MgV(*X*)0 catalysts were carried out as follows: after the desired temperature of reaction was reached, the reactor was maintained at this temperature for about 3 h, after which measurements were made. For the other samples, using the other experimental conditions, the same procedure was followed. A typical run, with the same charge of catalyst, lasted for about 12 h with three steps at 773, 793,

and 813 K. The reactor was also maintained at each temperature for about 3 h.

The possible existence of diffusion effects have also been considered. However, the catalysts have practically no microporosity (low surface areas and BET data). On the other hand, the porosity data for the present systems are similar to those observed in MoO_3 + α-Sb_2O_4. As in that case, no limitation due to internal diffusion was detected at similar flow rates and reaction rates (26). A limiting effect of internal diffusion has therefore to be ruled out.

In order to avoid preferential channelling in the catalytic bed, the ratio of the reactor bed/particle size should be greater than 10 (27). In our case this ratio is between 10 and 16.

2.6.2. Analysis of Reactants and Products

The reaction products were analyzed by on-line gas chromatography. An INTERSMAT IGC 121 ML chromatograph equipped with a catharometer was used. Analyses were automatically monitored by an integrator IGC-1D coupled to an electronic interface. For the study of MgV(X)0 catalysts, analyses were made using two columns: a stainless steel VZ-07 (20 ft × 1/8 in., 60/80 mesh, He carrier flow of 30 ml/min) for CO_2, propane, and propene and a washed molecular sieve 5A (6 ft × 1/8 in., 80/100 mesh, He carrier flow of 15 ml/min) for oxygen. The temperature of the furnace was 313 K. For tests with the other samples a stainless-steel Hayesep R column (1/8 in. × 6 ft 80/100 mesh, He carrier flow of 30 ml/min) was used to separate propane, propene, and CO_2 at a temperature of 343 K. The main products were propene and CO_2. Oxygen was not analyzed in these last tests. Traces of another product were detected situated after the peaks assigned to CO_2. This product could not be identified. No other oxygenate products was observed.

2.6.3. Expression of the Catalytic Activity

Catalytic activities are expressed as conversion of propane (C), selectivity (S), and yield (Y) of product as defined below:

$$C\% = \frac{\text{moles of propane consumed}}{\text{moles of propane in feed}} \times 100$$

$$Y\% = \frac{\text{moles of propene produced}}{\text{moles of propane in the feed}} \times 100$$

$$S\% = \frac{\text{moles of propene produced}}{\text{moles of propane consumed}} \times 100 = \frac{Y}{C} \times 100.$$

2.6.4. Expression of the Synergetic Effects

The kinetics of the various oxidation reactions have not been determined, because our objective was an approximate ranking of the various catalysts and the qualitative detection of synergy effects on the basis of measurements made in fixed conditions.

For simplification, we based the calculation of the synergetic effect on the simplified assumption of a zero order. This is an acceptable approximation for low conversions but cannot be expected to hold if a substantial transformation of propane occurs. Using these approximate values, the synergetic effect observed for the mechanical mixtures is expressed as the increase of conversion or yield compared to the properly weighted average values obtained for the components of the mixture when alone.

The synergetic effects are calculated by the formula

$$\text{Synergy effect} = \frac{X_{AB} - X_{(A+B)}}{X_{(A+B)}} \times 100,$$

where X_{AB} is the conversion, yield, or selectivity of the mixture and $X_{(A+B)}$ is the conversion, yield, or selectivity which would be observed in the absence of any synergetic effect, defined for a mixture with a given Rm as

$$C_{(A+B)} = Rm \times C_A + (1 - Rm) \times C_B,$$

$$Y_{(A+B)} = Rm \times Y_A + (1 - Rm) \times Y_B,$$

and

$$S_{(A+B)} = \frac{Rm \times Y_A + (1 - Rm) \times Y_B}{Rm \times C_A + (1 - Rm) \times C_B},$$

in which C_A and C_B are the propane conversion and Y_A and Y_B are the yield in propene of the samples A and B, respectively.

3. RESULTS

3.1. Sample Characterization

3.1.1. MgV(X) Oxides and the Mechanical Mixtures MMgV(X)MgV(Y) and MMgV(X)Sb

(*a*) *BET.* BET surface areas of the pure oxides are presented in Table 3. In general, the BET surface areas of the mixtures (obtained by 0, I, II, III, and IV sample condition preparation) are the same as those calculated using the formula in Section 2.3.3.

Within the precision limit of the BET method no difference between fresh and used catalysts can be detected for either pure oxides or mechanical mixtures.

(*b*) *XRD.* For catalyst MgV(1/2)0, the XRD pattern corresponds to β-MgV_2O_6 (ASTM file 34-13, Galy (28), and Parker and Cauley (29). A small amount of α-MgV_2O_6 (2Θ = 20.69 and 31.06) was observed. For MgV(2/2)0 catalyst, the XRD pattern corresponds to α-$Mg_2V_2O_7$

TABLE 3

BET Surface Areas (m^2/g) and Crystalline Phases for Fresh MgV(X)n and α-Sb_2O_4

Sample	Fresh	XRD crystalline phases
MgV(1/2)0	4.5	β-MgV_2O_6 + traces α-MgV_2O_6
MgV(2/2)0	7.6	α-$Mg_2V_2O_7$
MgV(2/2)I	4.9	α-$Mg_2V_2O_7$
MgV(2/2)II	3.4	α-$Mg_2V_2O_7$
MgV(2/2)III	3.4	α-$Mg_2V_2O_7$
MgV(3/2)0	5.2	$Mg_3V_2O_8$ + traces α- and β-$Mg_2V_2O_7$
MgV(3/2)I	16.0	$Mg_3V_2O_8$ + traces α-$Mg_2V_2O_7$
MgV(3/2)II	3.4	$Mg_3V_2O_8$ + traces α-$Mg_2V_2O_7$
MgV(3/2)III	8.7	$Mg_3V_2O_8$ + traces α-$Mg_2V_2O_7$
α-Sb_2O_4	0.7	Cervantite
α-Sb_2O_4	2.5	Cervantite

Note. X = Mg/V atomic ratio and n = 0, I, II, and III preparation conditions (Secton 2.2.1.b).

(ASTM file 31-816, Clarck (30)). No impurity was detected (see Fig. 1A and Table 3). MgV(2/2) I, II, III, and IV also show the XRD pattern of α-$Mg_2V_2O_7$ with slight impurities which could not be identified (see Fig. 1B). For MgV(3/2)0 catalyst, the XRD pattern corresponds to $Mg_3V_2O_8$ (ASTM file 37-351, Lubin (31)); small amounts of α- and β-$Mg_2V_2O_7$ are detected. The XRD pattern of MgV(3/2) I, II, III, and IV corresponds to that of $Mg_3V_2O_8$, with a percentage purity between 95% (I, IV) and 97% (II, III) (see Section 2.3.2) (see Fig. 1B and Table 3). The XRD pattern of the antimony oxide corresponds to that of α-Sb_2O_4 (cervantite). XRD patterns of the mechanical mixtures corresponded to the superposition of those observed for the individual pure catalysts. In the case of both pure oxides and mechanical mixtures, no change was observed in the position or the intensities of the peaks after reaction. No new peak was observed after test.

(*c*) *Vanadium oxidation state.* In both single and two phase catalysts, the average oxidation state of vanadium was +5, before and after catalytic test.

(*d*) *XPS.* Some remarks concerning the decomposition of the asymmetric V 2*p* peaks must be made before examining the XPS results.

(i) The reconstruction of the V 2*p* envelope using the constraints described in Section 2.3.3 leads to an incorrect fitting, which is evidenced by controlling the quality of the statistic parameter χ^2. The fitting is especially bad for the V $2p_{1/2}$ peak. This is a result of the strong influence of the O 1*s* (or O 1*s* + Sb $3d_{5/2}$) peak in background subtraction.

(ii) The reconstruction of the V 2*p* envelope (see Fig. 2), with no area and interval constraints, was carried out in order to achieve a better fitting and thus to calculate a more accurate quantity of total vanadium. In the following this quantity will be used to calculate XPS atomic ratios.

(iii) The binding energy value of 517.3 ± 0.2 eV for the V $2p_{3/2}$ peak observed for all catalysts corresponds to that found in the V_2O_5 standard. This value is also in agreement with literature data (32–35). Another V $2p_{3/2}$ peak, at

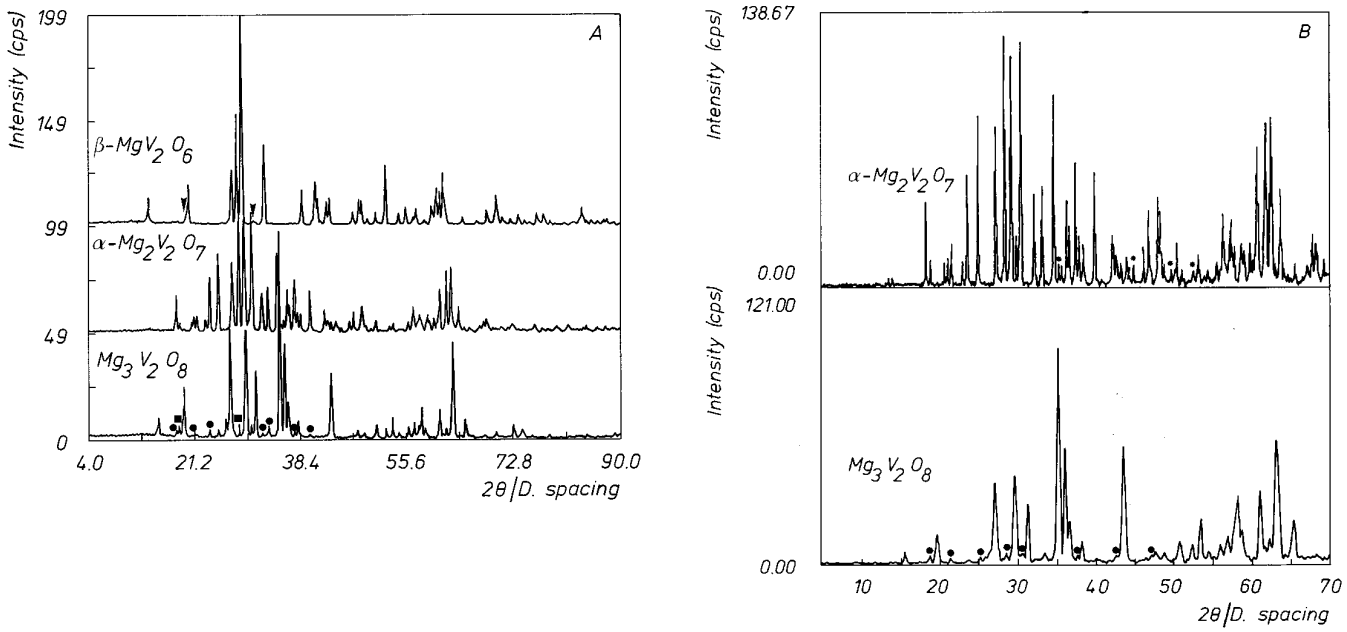

FIG. 1. (A) X-ray patterns of β-MgV_2O_6, α-$Mg_2V_2O_7$, and $Mg_3V_2O_8$. Impurities: ● α-$Mg_2V_2O_7$, ■ β-$Mg_2V_2O_7$, and ▼ α-MgV_2O_6. (B) X-ray patterns of $Mg_3V_2O_8$ and α-$Mg_2V_2O_7$. Impurities: ● α-$Mg_2V_2O_7$ and * not identified.

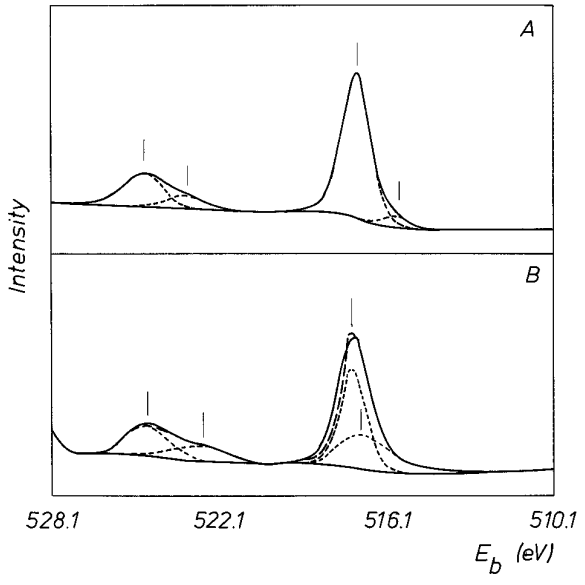

FIG. 2. XPS spectra of V 2*p* envelope with no area and interval constraints for (A) pretreated V_2O_5 and (B) MMgV(3/2)Sb(ia), *Rm* = 0.50, catalyst (see Section 2.3.3).

lower BE value, is also observed for all catalysts in the range 515.1–516.1 eV. This may be ascribed to V^{4+}. A similar BE range is reported in the literature (32, 36, 37) for this oxidation state. In spite of precautions taken in preparing the V_2O_4 standard (see Section 2.3.3), the most dominant peak is that of V^{5+}. This prevents the accurate determination of the position of V $2p_{3/2}$ of V^{4+}.

(iv) In spite of the fact that the BE separation between Mg 2*s* and V $2p_{3/2}$ peaks in greater than between Mg(Auger) and V $2p_{3/2}$ and that the Mg 2*s* atomic sensitivity factor is smaller (0.575) than that of Mg(Auger) (4.1), similar XPS V/Mg atomic ratios are obtained when using one or the other.

The following XPS results are obtained using the above considerations. Similar binding energy values of V $2p_{3/2}$, O 1*s*, Mg 2*s*, Mg(Auger), and Sb $3d_{3/2}$ are observed in all mechanical mixtures before and after test. These BE values correspond to those found in pure MgV(*X*) and α-Sb_2O_4 oxides (see Table 4A).

TABLE 4B

XPS Analysis: V/Mg Atomic Ratios for Pure MgV(*X*), and Bulk Atomic Ratio Are Indicated (See Section 2.3.3)

	V/Mg		
	XPS		
Sample	Fresh	Used	Bulk
MgV(1/2)	1.54	1.53	2.00
MgV(2/2)	0.73	0.88	1.00
MgV(3/2)	0.53	0.51	0.67

The XPS V/Mg atomic ratios are lower than those of the bulk (see Table 4B). Similar XPS V/Mg atomic ratios are found in MgV(*X*)0 and MgV(*X*)I oxides, before and after test. Slightly higher XPS V/Mg atomic ratios are observed after test for the MgV(2/2) catalyst.

For the mechanical mixtures MMgV(*X*)0MgV(*Y*) and MMgV(*X*)IIMgV(*Y*), the XPS V/Mg atomic ratios corresponded to the addition of those observed for pure catalysts (see Table 4B) and remained unchanged after reaction.

The XPS V/Mg, V/Sb, and Sb/(V + Mg + Sb) atomic ratios for the mechanical mixtures MMgV(*X*)ISb(ia) are presented in Tables 5A and 5B. Concerning MMgV(2/2)ISb(ia) (Table 5A), slightly higher XPS V/Mg atomic ratios are observed after test whereas the XPS V/Sb and Sb/(V + Mg + Sb) atomic ratios are close to those of the bulk. In the case of MMgV(3/2)ISb(ia) (Table 5B), the XPS V/Mg atomic ratios remain unchanged after test whereas the XPS V/Sb and Sb/(V + Mg + Sb) atomic ratios are different to those of the bulk. Similar results are obtained for the mechanical mixtures of MMg(*X*)0Sb.

The XPS C/V or C/Mg atomic ratios for all MMgV(*X*)0Sb and MMgV(*X*)ISb(ia) were also measured. The values are not reported because no change in these ratios was observed after test.

(*e*) *TEM and AEM.* TEM micrographs of MMgV(3/2)ISb(ia) with *Rm* = 0.50 before and after test are presented in Figs. 3A and 3B which can given an overview of

TABLE 4A

XPS Analysis: Binding Energies for V $2p_{3/2}$, O 1*s*, Mg 2*s*, Mg (Auger), and Sb $3d_{3/2}$ Peaks in Pure MgV(*X*)0, MgV(*X*)I, and α-Sb_2O_4 Oxides

Sample	BE (V $2p_{3/2}$)	BE (O 1*s*)	BE (Mg 2*s*)	BE (Mg Auger)	BE (Sb $3d_{3/2}$)
MgV(*X*)*n*	517.0 ± 0.2 516.0 ± 0.2	530.0 ± 0.2	89.5 ± 0.2	304.0 ± 0.2	
α-Sb_2O4					539.9 ± 0.2

TABLE 5A

XPS Results for V/Mg, V/Sb, and Sb/(V + Mg + Sb) Atomic Ratios for Fresh and Used MMgV(2/2)ISb(ia); Bulk Atomic Ratio (See Section 2.3.3) Is Also Indicated

	V/Mg			V/Sb			Sb/(V + Mg + Sb)		
	XPS			XPS			XPS		
Rm[a]	Fresh	Used	Bulk	Fresh	Used	Bulk	Fresh	Used	Bulk
0	—	—	—	—	—	—	—	—	—
0.25	0.99	1.05	1.00	0.48	0.23	0.39	0.50	0.69	0.41
0.50	0.76	0.84	1.00	1.18	0.89	1.17	0.23	0.34	0.30
0.75	0.87	1.00	1.00	3.48	3.42	3.51	0.12	0.12	0.12
1.0	0.73	0.88	1.00	—	—	—	—	—	—

[a] *Rm* is the mass ratio.

the arrangements of the two oxides (see also Table 6). The larger particles are α-Sb_2O_4. The smaller particles, spheres of about 0.05–0.1 μ, correspond to MgV(3/2)I (see Fig. 3A). The difference in particle sizes corresponds to the BET results. The pictures show that α-Sb_2O_4 crystallites are surrounded by MgV(3/2)I particles. Some MgV(3/2)I particles remain isolated.

AEM microanalyses were realized for the catalysts before and after test at different points of the samples. The results are essentially the same: isolated particles of α-Sb_2O_4 (point 1) and MgV(3/2)I (points 4, 5, 6, 7, 8).

3.1.2. MgV(X)III Impregnated with Antimony (MgV(X)III/L Catalysts

The BET surface areas and XPS results are reported in Tables 7A and 7B, respectively. It was verified that the solvent used for impregnation had no effect on the BET surface areas (see Table 7A).

An increase in the values of surface areas is observed after the MgV(*X*)III catalysts were impregnated with Sb ions, this increase being larger for higher α-Sb_2O_4 loadings. In addition, higher BET surface areas are developed by the impregnated catalysts after test.

Regarding XPS results, (see Table 7B), XPS V/Mg atomic ratios are lower than the bulk values. Higher XPS V/Mg atomic ratios are observed after test for MgV(2/2)III/*L* catalysts.

A similar tendency is observed regarding changes in XPS Sb/(V + Mg + Sb) atomic ratios for both MgV(2/2)III/*L* and MgV(3/2)III/*L* catalysts. An increase in this ratio with Sb content and a decrease of this ratio after test is observed. Regarding the MgV(2/2)III/1 catalyst no change in the XPS Sb/(V + Mg + Sb) atomic ratio is observed after test.

In all samples the XPS C/V atomic ratios show a decrease after test. When the antimony content is higher the decrease is more pronounced. The high XPS C/V atomic ratio for the MgV(3/2)III/3 catalyst before test can be due to a deficient washing of the sample and the fact that $CHCl_3$ had been used in the preparation was not well eliminated.

TABLE 5B

XPS Results for V/Mg, V/Sb, and Sb/(V + Mg + Sb) Atomic Ratios for Fresh and Used MMgV(3/2)ISb(ia); Bulk Atomic Ratio (See Section 2.3.3) Is Also Indicated

	V/Mg			V/Sb			Sb/(V + Mg + Sb)		
	XPS			XPS			XPS		
Rm	Fresh	Used	Bulk	Fresh	Used	Bulk	Fresh	Used	Bulk
0	—	—	—	—	—	—	—	—	—
0.25	0.52	0.57	0.67	1.11	0.90	0.34	0.23	0.29	0.53
0.50	0.48	0.49	0.67	3.57	2.48	1.02	0.08	0.12	0.29
0.75	0.42	1.44	0.67	5.88	6.43	3.05	0.05	0.04	0.11
1.0	0.53	0.51	0.67	—	—	—	—	—	—

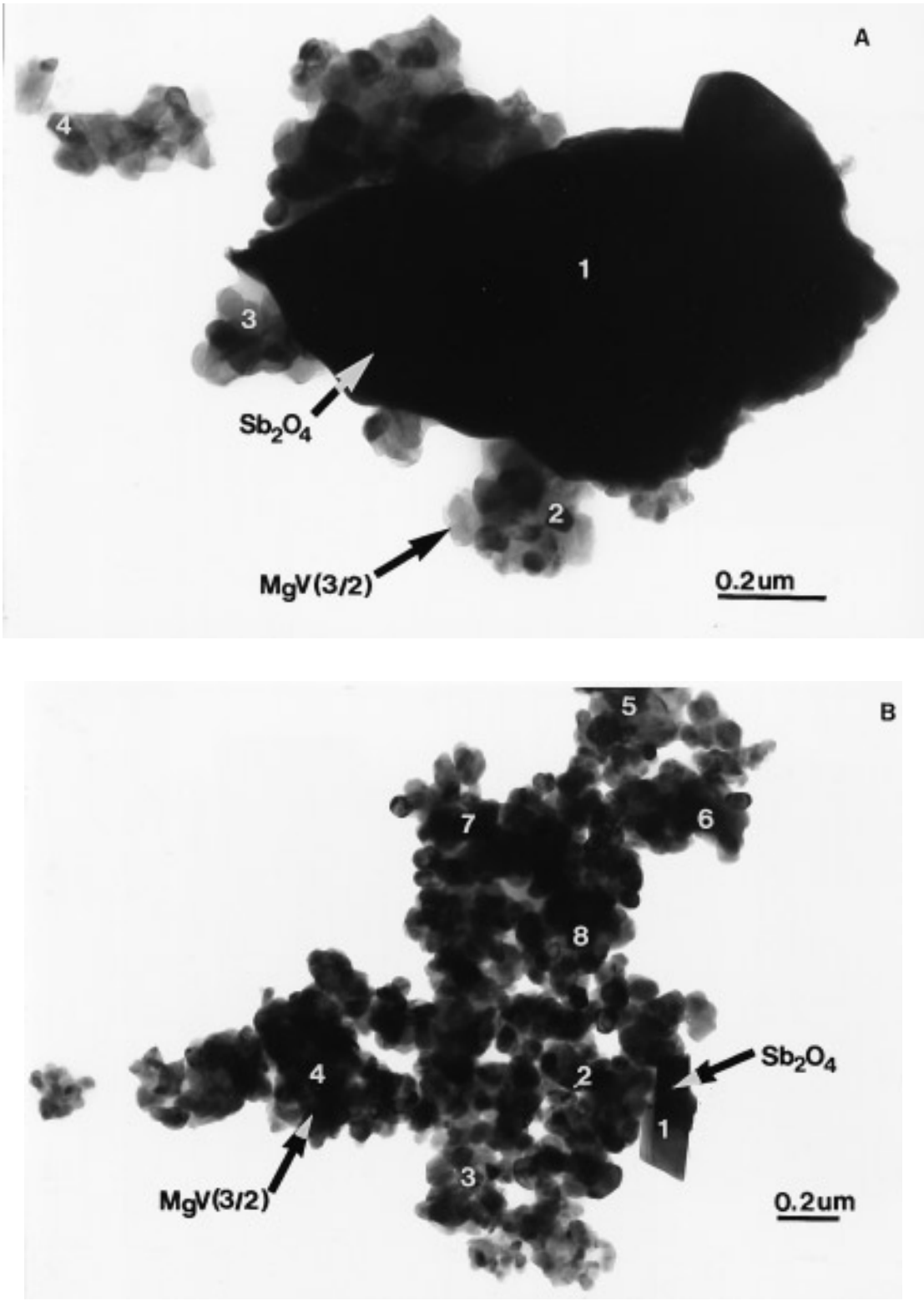

FIG. 3. TEM micrographs of MMgV(3/2)ISb(ia), $Rm = 0.50$, (A) before test and (B) after test.

TABLE 6

Analysis by Electron Microscopy of MMgV(3/2)Sb(ia) before and after Test

Point	Fresh		Used	
	Mg/Sb	V/Sb	Mg/Sb	V/Sb
1	1.2×10^{-2}	9.6×10^{-3}	0.1	0.2
2	4.9	10.0	18.6	42.4
3	2.3	6.2	56.9	107.5
4	27.4	53.0	∞	∞
5			54.6	100.3
6			234.0	508.0
7			415.0	946.5
7			274.6	665.0

Impregnated catalysts, either fresh or used, show only the XRD patterns corresponding to MgV(2/2) and MgV(3/2) oxides. No new peaks ascribed to other phases were observed.

3.1.3. Calcined Mechanical Mixtures of MMgV(X)IVSb with Rm = 0.5 (MMgV(X)IVSb/T Catalysts

For the MMgV(3/2)IVSb catalyst no new phase was detected by XRD even after 6 days calcination at 823 K. The presence of a new phase, $MgSb_2O_6$, was observed in the XRD patterns only after 2 days calcination at 923 K.

In the case of MMgV(2/2)IVSb the formation of $MgSb_2O_6$ was detected after only 1 day calcination at 823 K.

A change in color from yellow to grey is also observed for all samples in which the new phase was detected.

The binding energy values of V $2p_{3/2}$, O 1*s*, Mg (Auger), and Sb $3d_{3/2}$ are identical to those reported in Table 4A. The binding energy value of Sb $3d_{3/2}$ in $MgSb_2O_6$ is identical to that of α-Sb_2O_4.

The XPS V/Mg atomic ratio for MMgV/(2/2)IVSb/*T* catalysts (see Table 8A) is even lower than that of the noncalcined MgV(2/2)ISb(ia) catalyst with *Rm* = 0.5 (see Table 5A).

However, no difference in the XPS V/Mg atomic ratio is observed in MMgV(3/2)ISb/*T* catalysts at both 823 and 923 K (see Table 8B) compared to that of the noncalcined sample, MMgV(3/2)ISb(ia) (see Table 5B). No difference in the XPS V/Mg atomic ratio is observed after test for both MMgV(*X*)ISb/*T* catalysts (*X* = 2/2, 3/2).

The XPS C/V, C/Mg, and C/Sb atomic ratios for all MMgV(*X*)ISb/*T* were also measured. The values are not reported because no change in these ratios are observed after test.

For the sake of clarity, the XPS results for $MgSb_2O_6$ fresh and used and its mechanical mixture with α-Sb_2O_4

TABLE 7A

BET Surface Areas for Fresh and Used MgV(*X*)III Treated by $CHCl_3$ and Impregnated with Sb Ions, MgV(*X*)III/*L* Catalysts

Sample	S_{BET} (m^2/g)		Sample	S_{BET} (m^2/g)	
	Fresh	Used		Fresh	Used
MgV(2/2)III/$CHCl_3$	3.3	3.5	MgV(3/2)III/$CHCl_3$	8.7	9.1
MgV(2/2)III/1	3.0	3.4	MgV(3/2)III/1	9.5	10.3
MgV(2/2)III/3	3.8	4.0	MgV(3/2)III/3	10.4	10.7

Note. *X* = Mg/V atomic ratio and *L* is number of monolayers of Sb ions.

TABLE 7B

XPS Results for MgV(*X*)III/*L* Catalysts: V/Mg, V/Sb, Sb/(V + Mg + Sb), and C/V Atomic Ratios for Fresh and Used MgV(*X*)III/*L* Catalysts and Bulk Atomic Ratio (See Section 2.3.3) Are Indicated

Sample	V/Mg			Sb/(V + Mg + Sb)			C/V	
	Fresh	Used	Bulk	Fresh	Used	Bulk	Fresh	Used
MgV(2/2)III/1	0.69	0.82	1	0.07	0.08	0.01	2.46	1.83
MgV(2/2)III/3	0.75	0.82	1	0.19	0.10	0.02	3.21	1.76
MgV(3/2)III/1	0.45	0.49	0.67	0.19	0.14	0.01	2.81	1.97
MgV(3/2)III/3	0.47	0.54	0.67	0.40	0.24	0.05	7.19	2.36

TABLE 8A

XPS Results for MMgV(2/2)IVSb/*T* with *Rm* = 0.5 and V/Mg, V/Sb, and Sb/(V + Mg + Sb) Atomic Ratios for Fresh and Used Samples; Bulk Atomic Ratios (See Section 2.3.3), Calcination Temperature in K, and Calcination Time in Days Are Indicated

Temp. and calc. time	V/Mg			V/Sb			Sb/(V + Mg + Sb)		
	XPS			XPS			XPS		
	Fresh	Used	Bulk	Fresh	Used	Bulk	Fresh	Used	Bulk
823 K/1	0.38	—	1.00	0.85	—	1.17	0.24	—	0.30
823 K/2	0.38	0.39	1.00	0.85	0.84	1.17	0.24	0.25	0.30
823 K/6	0.39	—	1.00	0.86	—	1.17	0.25	—	0.30
923 K/2	0.36	0.39	1.00	0.83	0.83	1.17	0.24	0.25	0.30

(*Rm* = 0.5) are also presented in Table 8C. The XPS Sb/Mg atomic ratio is lower than that of the bulk in both the pure $MgSb_2O_6$ and its mechanical mixture with α-Sb_2O_4. For $MgSb_2O_6$, a significant increase in XPS C/Mg and C/Sb atomic ratios is observed after test. However, in the mechanical mixture these ratios regain the values observed in the fresh $MgSb_2O_6$ catalyst.

For MMgV(2/2)IVSb/*T* catalysts, the XPS V/Sb atomic ratios are similar to those found in noncalcined MMgV(2/2)ISb(ia) (*Rm* = 0.5) after test. The similarity in XPS Sb/(V + Mg + Sb) atomic ratios in both noncalcined, MMgV(2/2)ISb(ia), and calcined, MMgV(2/2)IVSb, is due to the low XPS V/Mg atomic ratio found in the calcined samples.

In MMgV(3/2)IVSb/*T* catalysts, the XPS V/Sb atomic ratios (see Table 8B) are similar to those of the noncalcined MMgV(3/2)ISb(ia) catalysts after test (*Rm* = 0.5) (see Table 5B). XPS Sb/(V + Mg + Sb) atomic ratio depicted by MMgV(3/2)IVSb/*T* is similar to that of the noncalcined MMgV(3/2)ISb(ia) (*Rm* = 0.5) (see Table 5B).

XPS V/Sb atomic ratio remain unchanged after test in both MMgV(3/2)IVSb/*T* and MMgV(2/2)IVSb/*T* catalysts, this ratio being higher and lower than that of the bulk for MMgV(3/2)IVSb/*T* and MMgV(2/2)IVSb/*T*, respectively.

3.2. NH_3 TPD Measurements (Acidity)

Table 9 shows the acidity distribution for MgV(3/2)0, MgV(2/2)0, and MgV(1/2)0, calculated as explained in Section 2.4. Maximum NH_3 TPD is observed at 448 K for MgV(1/2)0, at 451 K for MgV(2/2)0, and at 498 K for MgV(3/2)0.

The specific acidity (total acidity per m^2) for both oxides (Table 9) shows that the number of acid sites decreases in the following order: MgV(2/2)0 > MgV(1/2)0 > MgV(3/2). α-Sb_2O_4 does not possess any acidity.

For MMgV(*X*)0Sb mixtures (*X* = 1/2, 2/2, and 3/2), the maximum NH_3 TPD and the variation in the number of acid sites are the same as for pure catalysts. However, a 15% decrease in the number of acid sites is observed for MMgV(1/2)0Sb catalyst (*Rm* = 0.5), and a 40% decrease is observed for MMgV(2/2)0Sb and MMgV(3/2)0Sb catalysts (*Rm* = 0.5) compared to those of the pure MgV(*X*) (*X* = 1/2, 2/2, 3/2).

TABLE 8B

XPS Results for MMgV(3/2)IVSb/*T* with *Rm* = 0.5 and V/Mg, V/Sb, and Sb/(V + Mg + Sb) Atomic Ratios for Fresh and Used Samples; Bulk Atomic Ratios (See Section 2.3.3), Calcination Temperature in K, and Calcination Time in Days Are Indicated

Temp. and calc. time	V/Mg			V/Sb			Sb/(V + Mg + Sb)		
	XPS			XPS			XPS		
	Fresh	Used	Bulk	Fresh	Used	Bulk	Fresh	Used	Bulk
823 K/1	0.53	—	0.67	2.50	—	1.02	0.12	—	0.29
823 K/2	0.55	0.59	0.67	2.40	2.40	1.02	0.13	0.13	0.29
823 K/6	0.54	—	0.67	2.40	—	1.02	0.12	—	0.29
923 K/2	0.55	0.59	0.67	2.40	2.50	1.02	0.12	0.13	0.29

TABLE 8C

XPS Results for $MgSb_2O_6$ and Its Mechanical Mixture with α-Sb_2O_4: XPS Sb/Mg, C/Mg, and C/Sb Atomic Ratios for Fresh and Used Samples, and Bulk V/Mg Atomic Ratio Are Indicated (See Section 2.3.3)

	Sb/Mg						
	XPS			C/Mg XPS		C/Sb XPS	
Sample	Fresh	Used	Bulk	Fresh	Used	Fresh	Used
$MgSb_2O_6$	0.70	0.73	2.00	0.70	1.13	1.00	1.54
$MgSb_2O_6$ + α-Sb_2O_4	—	0.75	2.00	—	0.60	—	0.80

TABLE 9

Acidity Distribution and Total Acidity for MgVO Oxides

	Acidity force[a]			Total specific acidity[a]
Sample	Weak	Intermediate	Strong	
MgV(1/2)0	40	43	17	2.1
MgV(3/2)0	25	38	36	1.6
MgV(2/2)0	40	38	32	4.4

[a] See Section 2.4.

3.3. Thermoreduction

Results are presented in Fig. 4. α-Sb_2O_4 undergoes only very little reduction. MgV(2/2)0 catalyst exhibits the lowest induction time for the reduction whereas V_2O_5 presents both the highest rate of reduction and maximum reduction level (see Fig. 4A).

Compared to the MgV(3/2)0 catalyst, the Mg/V(2/2)0 exhibits both a higher rate of reduction and a maximum reduction level (see Fig. 4A).

In the case of the mechanical mixtures of $Rm = 0.5$, a significant increase in the relative weight change and in the maximum reduction level is noted compared to the pure catalysts (see Fig. 4B).

3.4. Catalytic Activity Measurements

Some remarks concerning the development of the experimental work must be pointed out before analyzing the catalytic results. This section will be organized as suggested in the literature.

Different sample preparations and catalytic conditions (see Sections 2.2.1.a, 2.6.1 and 2.6.2) were carried out in order to achieve a better understanding of the role played by MgV(X) oxides (X = 1/2, 2/2, and 3/2) in the OD of propane, according to the strategy proposed in the Introduction.

First, MgV(X)0 oxides and their mechanical mixtures,

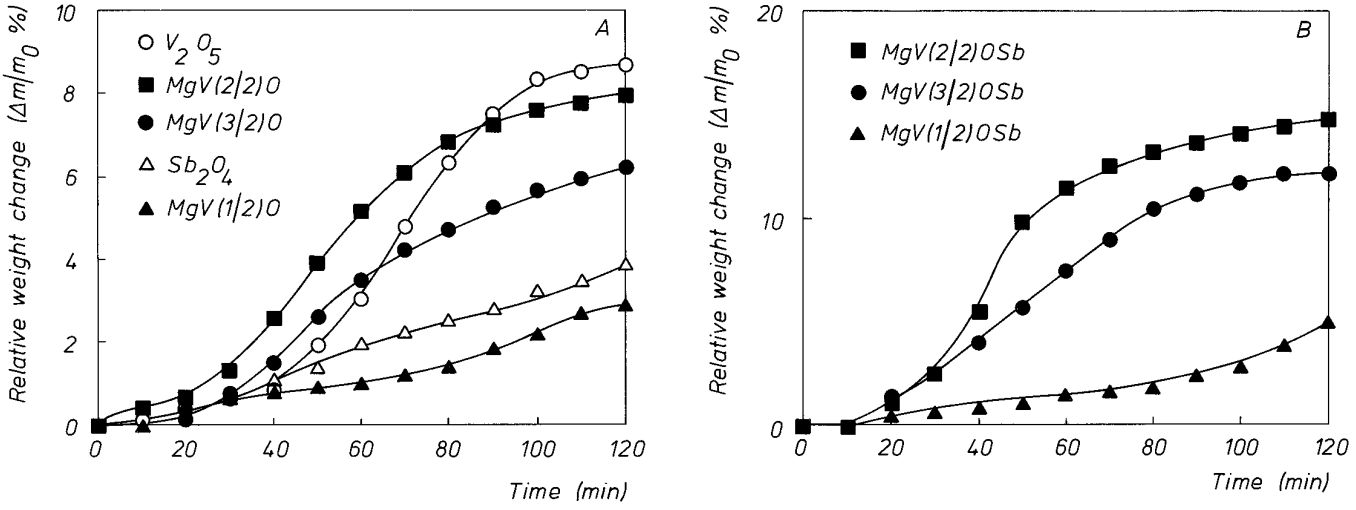

FIG. 4. Relative weight change % ($\Delta m/m_0$ %) versus time for (A) MgV(X)0 oxides, V_2O_5, and α-Sb_2O_4 and (B) MMgV(X)0Sb mechanical mixtures with $Rm = 0.5$. X = Mg/V atomic ratio.

TABLE 10

Catalytic Results: Conversion of Propane, Conversion of Oxygen, Selectivity to Propene, and Formation of CO_2 as a Function of vol% Oxygen and vol% Propane at 823 K for MgV(2/2)0 Catalyst

O_2/C_3H_8	O_2%	C_3H_8	C%	S%	C% (O_2)	Y% (CO_2)
1:1	8	8	9	71.4	10.2	1.1
2:1	16	8	10	70.0	8.5	19.5
3:1	24	8	14	67.8	3.9	22.0
1/1	8	8	9	71.4	10.2	15.1
2/1	8	4	7	69.7	10.3	17.5

MMgV(X)0MgV(Y), were tested in order to evaluate their activities in the OD of propane. MgV(2/2)0 and MgV (3/2)0 showed better performances for this reaction than MgV(1/2)0.

In a second series of experiments, the effect α-Sb_2O_4 had on the active phase in mixtures which contained MgV(X)0 with X = 2/2, 3/2 (MMgV(X)0Sb, Rm = 0.5) was also studied. The influence of the mixture composition (MMgV(X)IIMgV(Y) catalysts) and of both the agitation method and the mixture composition (MMgV(X)ISb(ia) catalysts) on the catalytic activities were also studied.

Finally, the possible tendency of contamination and formation of a new phase were studied, in samples of MgV(X)III (X = 2/2, 3/2) contaminated artificially with Sb ions (MgV(X)III/L catalysts) and in mechanical mixtures of MgV(X)IV (X = 2/2, 3/2) and α-Sb_2O_4 calcined at high temperatures for several days (MMgV(X)IVSb/T catalysts).

3.4.1. Preliminary Results

(*a*) *Influence of the partial pressure of oxygen propane.* Tests were carried out with the MgV(2/2)0 catalyst (200 mg) using either different oxygen/propane mole ratios (1/1, 2/1, and 3/1 with 8 vol% propane in the feed) or different propane/oxygen mole ratios (1/1 and 2/1 while maintaining the oxygen concentration constant at 8 vol%) at 823 K (see Table 10). The results in Table 10 show that when the O_2/propane molar ratio increases the conversion of propane and the yield of CO_2 increase. Simultaneously the conversion of oxygen and the selectivity to propene decrease. O_2/C_3H_8 values in the range 2.7–3.0 were selected for the catalytic tests (see Tables 10, 11 and 12).

(*b*) *Activity as a function of the mass of catalyst.* Figures 5A and 5B show the trends for the conversion and selectivity for the single phases, MgV(X)0 (X = 1/2, 2/2, 3/2), as a function of the amount of catalyst (70, 100, and 200 mg). Figure 5A shows that the conversion is not a linear function of the mass of catalyst.

All the MgV(X)0 catalysts show a variation of 8% in the conversion while approximate constant values are observed for the selectivity.

(*c*) *Activity as a function of the reaction temperature.* The evolution of catalytic activities were followed as a function of reaction temperature for both single- and two-phase catalysts, prepared in the conditions denoted by I, II, and III. The results reported in Tables 11 and 12 also include, for the sake of clarity, catalytic activities of MgV(X)0 and MMgV(X)0Sb (Rm = 0.5) at 823 K. Results will be discussed in 3.4.2.

(*d*) *Influence of sample preparation method.* Similar trends in catalytic activities (conversion) are observed for both, MMgV(2/2)ISb and MMgV(2/2)ISb(ia) mechanical mixtures but the highest conversion is observed for the mechanical mixtures prepared by intensive agitation (see Section 2.2.2.b). The better interdispersion between both oxides in these samples has been corroborated by electron microscopy observations. For this reason only, the catalytic activity results of MMgV(X)ISb(ia) are presented in Table 12. Results will be discussed in 3.4.2.

3.4.2. Single Phase Catalysts

Table 11 shows a decrease in propane conversion in the order MgV(3/2)0 > MgV(1/2)0 > MgV(2/2)0, whereas the selectivity to propene decreases in the order MgV(2/2)0 > MgV(1/2)0 > MgV(3/2)0; propene yield remains approximately the same for the three catalysts.

A comparison between MgV(3/2)I and MgV(2/2)I catalysts shows that propane conversion and propene yield are higher for MgV(3/2)I. In contrast, selectivity is higher for MgV(2/2)I. The catalytic activity trend exhibited by MgV(X)II catalysts is opposite to that observed in MgV(X)I catalysts. Regarding MgV(X)III catalysts, propane conversion is similar for both MgV(2/2)III and MgV(3/2)III, the propene yield and selectivity to propene being higher for MgV(3/2)III.

An important point to note is that MgV(2/2) catalysts show a higher selectivity to propene than MgV(3/2) catalysts only when the conversion of propane is low (10%). At higher conversion the selectivities are approximately the same.

3.4.3. Biphase Catalysts—Mechanical Mixtures

(*a*) *MMgV(X)ISb(ia) and MMgV(X)0Sb mechanical mixtures.* The results presented in Table 12 show that α-Sb_2O_4 modifies the performance of the pure MgV(X) catalysts.

MMgV(2/2)ISb(ia) mechanical mixtures (see Table 12A) show an important synergy effect in the conversion for all Rm. Maximum conversion is detected for Rm =

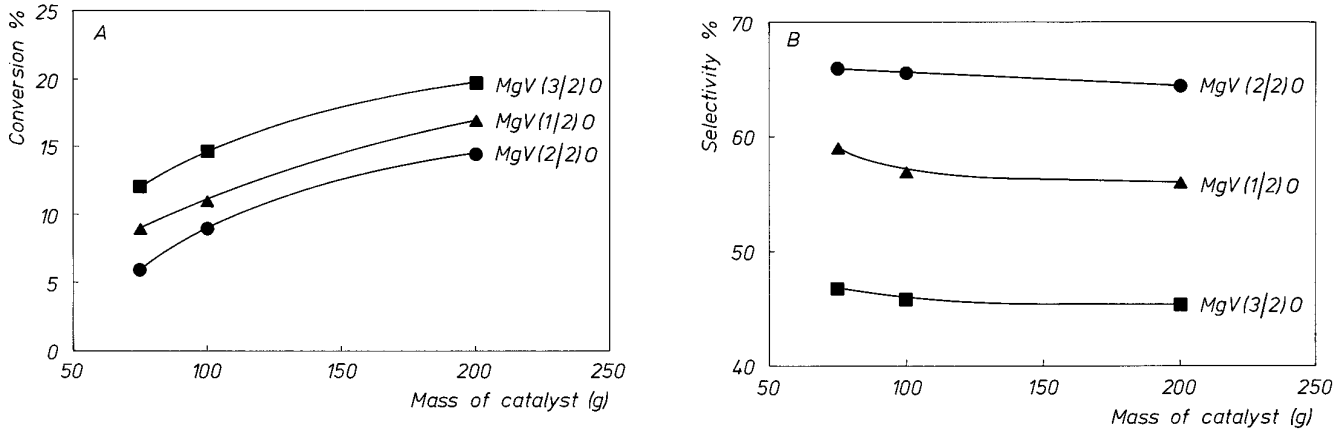

FIG. 5. (A) Conversion as function of the mass of catalyst and (B) selectivity as function of the mass of catalyst for MgV(X)0 (X = 1/2, 2/2, 3/2).

0.5, but the most important synergy is observed at Rm = 0.25, the intensity of this effect decreasing as the temperature increases. Regarding the yield, an important synergy effect is also observed at Rm = 0.25 and to a lesser extent at Rm = 0.5. In contrast, a synergy effect in the selectivity to propene is observed for all Rm.

Similar trends in catalytic behavior are observed with MMgV(2/2)0Sb (see Table 12B) where only an experiment with Rm = 0.5 has been done.

MMgV(3/2)ISb(ia) mechanical mixtures show a decrease in the conversion, namely no synergy effect for all Rm, except for Rm = 0.25 at 813 K. The intensity of this effect slightly decreases with increasing temperature. No synergy effect in the yield is observed, except for Rm = 0.25. However, a synergy effect in the selectivity to propene is observed for all Rm.

Both MMgV(3/2)0Sb and MMgV(3/2)ISb(ia) with Rm = 0.5 show similar trends.

In conclusion, an activity promotion is observed in the MMgV(2/2)Sb system at the expense of selectivity whereas the MMgV(3/2) system exhibits an increase in selectivity by suppression of unselective reactions.

(*b*) *MMgV*(X)*IIMgV*(Y) *and MMgV*(X)*0MgV*(Y) *mechanical mixtures*. In MMgV(3/2)IIMgV(2/2) (Table

TABLE 11

Catalytic Results: Conversion, Yield, and Selectivity of MgV(X)*n* Oxides

Sample	Weight (mg)	773 K			793 K			813 K			823 K		
		C%	Y%	S%	C%	Y%	S%	C%	Y%	S%	C%	Y%	S%
Mg/V(1/2)0	100										11.0	6.3	57.0
Mg/V(1/2)0	200										17.0	9.5	56.0
Mg/V(2/2)0	100										9.0	5.9	65.5
Mg/V(2/2)0	200										14.5	9.3	64.5
Mg/V(2/2)I(ia)	500	2.7	3.1	100	5.5	4.3	77.8	10.6	6.7	63.5			
Mg/V(2/2)II	1000	41.3	6.2	15.1	46.5	6.2	13.3	51.9	6.2	12.0			
Mg/V(2/2)II	500	4.2	1.7	40.8	5.1	2.4	47	7.9	3.7	46.8			
Mg/V(2/2)III	500	4.5	2.8	62.0	6.2	3.7	59.3	8.6	4.7	54.8			
Mg/V(3/2)0	100										14.6	6.7	45.8
Mg/V(3/2)0	200										19.7	8.9	45.3
Mg/V(3/2)I(ia)	500	12.4	5.6	45.6	15.0	7.6	50.2	20.1	9.4	46.7			
Mg/V(3/2)II	1000	8.7	0.9	9.5	9.5	1.5	15.7	10.7	3.0	28.2			
Mg/V(3/2)III	500	29.9	6.1	20.5	39.1	7.7	19.7	47.4	8.5	17.9			

Note. n = 0, I, II, and III preparation conditions. Experimental conditions for (a) MgV(X)0 samples: partial pressures of propane, oxygen and helium, 60.8, 182.4, and 516.8 Torr. $O2/C_3H_8$ = 3.0, total feed 37 ml/min and range of the rate of reaction of 2.38×10^{-7}–3.82×10^{-7} mole s^{-1} m^{-2} (see Section 2.6.1) and for (b) MgV(X)n (n = I, I, III), 42.4, 114.6, and 603 Torr. O_2/C_3H_8 = 2.7, total feed 33 ml/min and range of the rate of reaction of 1.38×10^{-8}–1.90×10^{-7} mol s^{-1} m^{-2} (see Section 2.6.1). 1 Torr = 133.3 N m^{-2}.

TABLE 12A

Catalytic Results: Conversion, Yield, and Selectivity to Propene and CO_2 Formation of MMgV(X)ISb(ia)

Sample	*Rm*	773 K C%	773 K Y%	773 K S%	773 K CO_2	793 K C%	793 K Y%	793 K S%	793 K CO_2	813 K C%	813 K Y%	813 K S%	813 K CO_2
MMgV(2/2)ISb(ia)	0.25	8.2	4.2	51.0	11.8	20.2	6.8	33.8	22.8	29.9	7.7	27.8	34.8
		(0.7)	(0.8)	(114)		(1.4)	(1.1)	(78.6)		(2.6)	(1.7)	(65.4)	
		1071	425	−55		1920	518	−57		1050	353	−57.5	
	0.50	13.0	4.8	36.5	16.4	22.2	6.1	27.3	29.0	33.5	6.5	19.4	51.9
		(1.4)	(1.5)	(107)		(2.7)	(2.1)	(77.8)		(5.3)	(3.3)	(62.3)	
		828	220	−68		722	190	−65		532	97	69	
	0.75	13.6	2.4	14.6	13.8	17.4	3.0	14.9	13.7	29.5	4.0	12.8	32.3
		(2.1)	(2.3)	(109)		(4.1)	(3.2)	(78.0)		(7.9)	(5.0)	(63.3)	
		1150	4.3	−87		324	−6.0	−81		273	−20	−80	
MgV(2/2)I(ia)	1.00	2.8	3.1	100	2.0	5.5	4.3	77.8	3.2	10.6	6.7	63.5	5.5
MMgV(3/2)ISb(ia)	0.25	1.4	1.3	91.8	1.0	2.8	2.5	90.2	1.8	7.6	5.7	75.4	3.5
		(3.1)	(1.4)	(45.2)		(3.7)	(1.9)	(51.3)		(5.0)	(2.3)	(46.0)	
		−55	−7	103		−24	32	76		52	148	64	
	0.50	3.5	2.1	60.6	1.2	4.3	2.9	68.2	1.7	6.9	4.0	57.7	2.7
		(6.2)	(2.8)	(45.2)		(7.5)	(3.8)	(50.7)		(10.0)	(4.7)	(47.0)	
		−43.5	−25	34		43	−24	34.5		−31	−15	23	
	0.75	4.4	3.5	80.0	3.0	5.9	5.0	85.5	5.1	10.1	6.6	65.8	8.3
		(9.3)	(4.2)	(45.2)		(11.2)	(5.7)	(50.9)		(15.1)	(7.0)	(46.3)	
		−53	−17	77		−47	−12	68		−33	−6	42	
MgV(3/2)I(ia)	1.00	12.4	5.6	45.6	7.4	15.0	7.6	50.2	10.8	20.1	9.4	46.7	15.3

Note. In parenthesis are the theoretical values in absence of synergy (see Section 2.6.4) and underlined, synergy effect (see Section 2.6.4). Experimental conditions: partial pressures of propane, oxygen, and helium, 42.4, 114.6, and 603 Torr. $O_2/C_3H_8 = 2.7$, total feed 33 ml/min and range of rates of reaction of 7.78×10^{-9}–2.43×10^{-7} mol s^{-1} m^{-2} (see Section 2.6.1).

13A), moderate positive synergy effects are observed in the conversion and in the yield. The synergy effect is more pronounced in the conversion at $R = 0.75$ and in the yield at $Rm = 0.5$. A significant increase of selectivity is observed for $Rm = 0.5$.

The results obtained with MMgV(X)0MgV(Y) ($Rm = 0.5$) and the pure phase (MgV(X)0) are presented in Table 13B. MMgV(3/2)0MgV(2/2) catalysts show similar trends to those observed with MMgV(3/2)IIMgV(2/2). However, no effects are observed in selectivity or conversion for MMgV(2/2)0MgV(1/2) or MMgV(3/2)0MgV(1/2), respectively.

3.4.4. Biphasic Catalysts—Impregnated Catalysts

The results are presented in Tables 14A and 14B. At 773 K, the conversion and yield values of MgV(2/2)III/1 catalyst compared to the nonimpregnated MgV(2/2)III catalyst show a decrease, however, the selectivity is higher.

Concerning MgV(3/2)III/L, there is a continuous decrease in the conversion and yield values with increasing Sb loading; the selectivity value shows an increase at low Sb loading, whereas values similar to those of the nonimpregnated MgV(3/2)III catalyst are observed at high Sb loading.

TABLE 12B

Catalytic Results: Conversion, Yield, and Selectivity to Propene and CO_2 Formation of MMgV(X)0Sb at 823 K

Sample	*Rm*	823 K C%	823 K Y%	823 K S%	823 K CO_2
MMgV(2/2)0Sb	0.50	20.5	12.2	60.0	5.7
		(4.5)	(3.0)	(67.0)	(0.6)
		355	307	−10	
MgV(2/2)0	1.00	9.0	5.9	65.5	1.2
MMgV(3/2)0Sb	0.50	9.5	6.1	64.0	0.3
		(7.3)	(3.3)	(45.0)	(0.2)
		30	85	42	
MgV(3/2)0	1.00	14.6	6.7	45.8	0.5

Note. In parenthesis are the theoretical values in absence of synergy (see Section 2.6.4) and underlined, synergy effect (see Section 2.6.4). Experimental conditions: 60.8, 182.4, and 516.8 Torr. $O_2/C_3H_8 = 3.0$, total feed 37 ml/min and range of rates of reaction of 2.38×10^{-7}–4.64×10^{-7} mol s^{-1} m^{-2} (see Section 2.6.1). 1 Torr = 133.3 N m^{-2}.

TABLE 13A

Catalytic Results: Conversion, Yield, and Selectivity to Propene of MMgV(X)IIMgV(Y)

Sample	*Rm*	773 K				793 K				813 K			
		C%	Y%	S%	CO_2%	C%	Y%	S%	CO_2%	C%	Y%	S%	CO_2%
MgV(2/2)II	0.00	41.3	6.2	15.1	48.3	46.5	6.2	13.3	53.4	51.9	6.2	12.0	62.1
MgV(3/2)IIMgV(2/2)	0.25	38.4	5.7	14.9	47.7	47.5	7.0	14.8	60.1	53.7	7.5	13.9	71.0
		(33.1)	(4.9)	(14.8)	(37.5)	(37.2)	(5.0)	(13.4)	(47.4)	(41.6)	(5.4)	(13.0)	(49.6)
		16	16	1	27	28	40	10	27	29	39	6.5	43
MgV(3/2)IIMgV(2/2)	0.50	29.0	5.5	19.0	20.7	34.2	7.0	20.5	28.8	37.1	7.6	20.6	35.8
		(25.0)	(3.5)	(14.0)	(27.8)	(28.0)	(3.8)	(13.7)	(31.3)	(23.9)	(4.6)	(19.2)	(37.2)
		16	57	33	−25	22	84	50	−8	55	65	7	−4
MgV(3/2)IIMgV(2/2)	0.75	27.4	3.1	11.3	25.9	29.4	3.9	13.4	28.4	35.9	5.4	15.1	37.7
		(16.8)	(2.2)	(13.1)	(17.8)	(18.7)	(2.7)	(14.4)	(36.3)	(21.0)	(3.8)	(18.1)	(24.7)
		63	41	−14	8	57	44	−7	6	71	42	−17	51
MgV(3/2)II	1.00	8.7	0.9	10.7	7.2	9.5	1.5	15.7	9.1	10.7	3.0	28.2	12.3

Note. In parenthesis are the theoretical values in absence of synergy (see Section 2.6.4) and underlined, synergy effect (see Section 2.6.4). Experimental conditions: partial pressures of propane, oxygen, and helium, 42.4, 114.6, and 603 Torr. O_2/C_3H_8 = 2.7, total feed 33 ml/min and range of rates of reaction of 1.97×10^{-7}–2.75×10^{-6} mol s^{-1} m^{-2} (see Section 2.6.1).

In spite of the notably lower Sb content (between 1% and 10%) of the impregnated catalyst compared to that of the mechanical mixtures (between 25% and 75%), similar synergy effects are observed in both types of catalysts (see Tables 12 and 14).

TABLE 13B

Catalytic Results: Conversion, Yield, and Selectivity to Propene of MMgV(X)0MgV(Y) at 823 K

Sample	*Rm*	823 K			
		C%	Y%	S%	CO_2%
MgV(1/2)0		17.0	9.5	56.0	2.5
MgV(2/2)0		14.5	9.3	64.5	2.5
MgV(3/2)0		19.7	8.9	45.3	3.5
MgV(2/2)0MgV(1/2)	0.50	21.0	9.0	43.0	3.9
		(15.7)	(9.4)	(59.9)	(2.5)
		33.7	−4.2	−28	56
MgV(3/2)0MgV(1/2)	0.50	16.5	9.3	56.7	2.6
		(18.3)	(9.1)	(49.7)	(2.5)
		−9.8	2	−14	4
MgV(3/2)0MgV(2/2)	0.50	15.9	11.6	73.2	2.9
		(17.1)	(9.1)	(53.2)	(3.0)
		−7	29	37	−3

Note. In parenthesis are the theoretical values in absence of synergy and underlined, synergy effect. Experimental conditions: partial pressures of propane, oxygen, and helium, 60.8, 182.4, and 516.8 Torr. O_2/C_3H_8 = 3.0, total feed 37 ml/min and range of rates of reaction of 1.91×10^{-7}–3.5×10^{-7} mol s^{-1} m^{-2}. 1 Torr = 133.3 N m^{-2}.

3.4.5. Biphasic Catalysts—Calcined MMgV(X)IVSb/T Mixture

The catalytic results at 813 K are presented in Table 15 for both noncalcined, MMgV(X)IVSb, and calcined, MMgV(X)IVSb/823/6, catalysts (X = 2/2, 3/2). MMgV(2/2)IVSb/823/6 shows an important increase in the conversion and in the CO_2 production (decrease of selectivity to propene) compared to the noncalcined catalyst. Regarding MMgV(3/2)IVSb/823/6, an increase in the conversion and in the CO_2 production is also observed and this is accompanied by an increase in the selectivity to propene.

3.4.6. $MgSb_2O_6$ and $MgSb_2O_6$ + α-Sb_2O_4 Mixture

Only the presence of CO_2 was detected in the products of the reaction during the catalytic test of $MgSb_2O_6$. Compared to pure $MgSb_2O_6$ (propane conversion of 7% and CO_2 formation of 19%), the mechanical mixture with α-Sb_2O_4 shows an increase of 70% in the propane conversion and an increase of 80% in CO_2 formation.

4. DISCUSSION

The above activity results show that synergetic effects are observed in both MMgV(2/2)MgV(3/2) and MMgV(X)Sb (X = 2/2, 3/2) catalysts when tested in the OD of propane to propene.

The aim of this study is to determine if the remote control mechanism can explain the observed synergetic effects. However, it is known that several solid-state processes can take place when two oxides are mixed together;

TABLE 14A

Catalytic Results: Conversion, Yield, and Selectivity of Impregnated MgV(2/2)III Oxides with Sb ions, MgV(2/2)III/*L*

	773 K				793 K				813 K			
Sample	C%	Y%	S%	CO_2	C%	Y%	S%	CO_2	C%	Y%	S%	CO_2
MgV(2/2)III	4.5	2.8	62.0	1.6	6.2	3.7	59.3	2.4	8.6	4.7	54.8	3.4
MgV(2/2)III/1	2.6	1.9	72.8	0.8	5.5	2.9	53.0	1.7	6.9	4.1	59.5	3.1
MgV(2/2)III/3	22.97	4.8	20.9	28.5	35.1	6.1	17.2	42.3	45.7	6.5	14.2	55.8

Note. Experimental conditions: partial pressures of propane, oxygen, and helium of 42.4, 114.6, and 603 Torr. O_2/C_3H_8 = 2.7, total feed 33 ml/min and range of rates of reaction of 2.17×10^{-8}–3.0×10^{-7} mol s^{-1} m^{-2} (see Section 2.6.1). 1 Torr = 133.3 N m^{-2}.

i.e., the formation of a new phase, contamination between the oxides, coke deposition, sintering, etc. There are consequently, a priori, different explanations to the synergetic effects observed in the different catalysts studied.

The first part of the discussion will therefore examine the results of catalyst physicochemical characterization. The possible mechanisms involved in the observed synergetic effects will be discussed in the second part.

4.1. Single-Phase Catalysts

4.1.1. MgV(2/2) Catalysts

This catalyst is practically pure α-magnesium pyrovanadate (α-$Mg_2V_2O_7$). No phase modification and no change in BET surface area or bulk and surface oxidation state have been detected after catalytic tests.

Only, a slight increase in XPS V/Mg atomic ratios is observed. This can be due to V_2O_5 segregation at the surface. V_2O_5 can be segregated as crystallites or by the form of monolayer. The absence of changes in BET surface areas suggests that the monolayer form is more likely. Crystallites would contribute by adding surface areas.

4.1.2. MgV(3/2) Catalysts

Fresh catalyst consists principally of $Mg_3V_2O_8$ with slight impurities of α-$Mg_2V_2O_7$ (between 3% and 5%). This is due to the fact that a transition through α-$Mg_2V_2O_7$ is necessary to obtain $Mg_3V_2O_8$. More drastic calcination conditions (time and temperature) would be required to obtain $Mg_3V_2O_8$ with a high degree of purity, but in such conditions very low BET surface areas would be obtained (see Table 1). No change in catalyst structure or bulk and surface oxidation state is observed after test.

It must be pointed out that for both MgV(2/2) and MgV(3/2), XPS V/Mg atomic ratios are lower than those of the bulk (see Section 2.3.3).

4.2. Biphasic Catalysts

4.2.1. Coke Deposition and Sintering

In this discussion we shall examine two parameters which could potentially explain some of the observed phenomena. These are deposition of coke and sintering.

There is no deposition of coke on α-Sb_2O_4. Preferential coke deposition on MgV(X) oxides (X = 2/2, 3/2) is ex-

TABLE 14B

Catalytic Results: Conversion, Yield, and Selectivity of Impregnated MgV(2/2)III Oxides with Sb ions, MgV(3/2)III/*L*

	773 K				793 K				813 K			
Sample	C%	Y%	S%	CO_2	C%	Y%	S%	CO_2	C%	Y%	S%	CO_2
MgV(3/2)III	29.9	6.1	20.5	32.7	39.1	7.7	19.7	45.4	47.4	8.5	17.9	59.1
MgV(3/2)III/1	11.2	3.2	28.3	15.8	18.3	4.3	23.5	26.1	26.2	5.8	22.2	26.1
MgV(3/2)III/3	6.7	1.2	18.6	8.0	17.7	3.7	21.0	20.6	28.8	5.4	18.6	20.6

Note. Experimental conditions: partial pressures of propane, oxygen, and helium of 42.4, 114.6, and 603 Torr. O_2/C_3H_8 = 2.7, total feed 33 ml/min and range of rates of reaction of 1.61×10^{-8}–1.36×10^{-7} mol s^{-1} m^{-2} (see Section 2.6.1).

TABLE 15

Catalytic Results: Conversion, Selectivity, and CO_2 Production of Calcined Samples MMgV(X)IVSb/823/6 (X = 2/2, 3/2) with Rm = 0.5 at 813 K

Sample		C%	S%	CO_2%
MMgV(2/2)IVSb	noncalcined	2.3	>90	0.9
	calcined	22.4	26.2	14.4
MMgV(3/2)IVSb	noncalcined	2.2	15.8	2.9
	calcined	9.7	32.4	13.2

Note. Experimental conditions: partial pressure of propane, oxygen, and helium: 42.4, 114.6, and 603 mm Hg. O_2/C_3H_8 = 2.7, total feed 33 ml/min and range of rates of reaction of 1.45×10^{-8}–2.8×10^{-8} mol s^{-1} m^{-2} (see Section 2.6.1).

cluded because the XPS C/V (or C/Mg) atomic ratios and BET surface areas remain nearly constant during test for MMgV(X)Sb mixtures. On the other hand, the XPS C/V (or C/Mg) atomic ratios diminish after the test in the catalysts prepared by impregnation. This indicates that, even if a deposition of coke took place, carbon would be eliminated during reaction.

Sintering is also excluded in MMgV(X)Sb because no decrease in BET surface area is observed after the test.

This is particularly true for MMgV(3/2)Sb mixtures, where the large contribution of MgV(3/2) to BET surface area would make easily detectable a sintering of this phase.

In MMgV(2/2)Sb, other phenomena that take place during the test could compensate a hypothetical decrease in BET surface areas. This will be discussed below.

4.2.2. Formation of a New Phase or a Solid Solution. Surface Contamination

(*a*) *MMgV(2/2)MgV(3/2) System.* The study of the mixtures of the two vanadates, MMgV(2/2)MgV(3/2), reveals neither a formation of a new phase nor contamination. This is logical for the first possibility. The second observation indicates that there is no preferential migration of one element from one phase to the other. This is also logical because both oxide phases contain the same metallic atoms in almost the same ratio.

(*b*) *MMgV(X)Sb (X = 2/2, 3/2) systems.* We begin by discussing the case of samples containing MgV(3/2). X-ray diffraction measurements did not indicate the formation of a new phase either after catalytic test with the mixtures MMgV(3/2)ISb(ia) or after calcination for 6 days at 823 K with the mixtures MMgV(3/2)IVSb. No change in the BET surface areas or sample colors after test or calcination was observed.

Only in the case of MMgV(3/2)IVSb where calcination had been performed for 2 days at 923 K could traces of a new phase, i.e., $MgSb_2O_6$, be detected and a change of color observed. These conditions are very far from those used under catalytic reaction. At any rate, if $MgSb_2O_6$ was formed during the test, this would be only a very small amount.

In MMgV(3/2)ISb(ia) mixtures, the low XPS Sb/(V + Mg + Sb) and the high XPS V/Sb atomic ratios compared to those of the bulk have to be explained. We show below the reasons which indicate that is due to the difference in particle size between MgV(3/2)I and α-Sb_2O_4 (S_{BET} MgV(3/2)I = 16.0 m^2/g and S_{BET} α-Sb_2O_4 = 0.7 m^2/g).

Indeed, when two phases are mixed, the XPS surface composition depends on the difference of particle size between the phases, the aggregation of the particles, and mutual arrangements between the particles of one phase and the particles of the other phase (13). Here, the aggregation of the particles has been minimized, by using a vigorous agitation during preparation, and the effect can not be attributed to preferential aggregation or special mutual arrangement.

In principle, the lower XPS Sb/(V + Mg + Sb) and the higher XPS V/Sb atomic ratios compared to those of bulk might also be explained by a contamination of α-Sb_2O_4 by MgV(3/2)I. But this assumption must be discarded because of the similarity of XPS Sb/(V + Mg + Sb) and XPS V/Sb atomic ratios before and after the test. If a contamination at room temperature existed, it is highly improbable that it would remain stable after the sample has been tested at 813 K.

On the other hand, the XPS Sb/(V + Mg + Sb) and the XPS V/Sb atomic ratios are close to those of bulk in MMgV(2/2)ISb(ia) catalysts, in which the difference in particle size MgV(2/2)I and α-Sb_2O_4 is only small (S_{BET} MgV(2/2)I = 4.9 m^2/g and S_{BET} α-Sb_2O_4 = 2.5 m^2/g.).

For these reasons we retain the difference in particle size as the reason of the low values of XPS Sb/(V + Mg + Sb) and the high values of XPS V/Sb atomic ratios compared to those of the bulk.

AEM analyses suggest that MgV(3/2)I has not been contaminated by Sb ions during the catalytic reaction. In fact, the AEM analysis is the same before and after reaction. In both cases isolated particles of α-Sb_2O_4 and MgV(3/2)I were observed. The fact that the AEM Mg/Sb and V/Sb peak intensity ratios are not the same for all the particles is explained by the influence of the neighborhood over the Sb particles. Thus, a contamination seems to be excluded. The principal argument to exclude the contamination is that the same AEM results are observed for the fresh and used samples. In both cases, pure MgV(3/2)I and α-Sb_2O_4 particles are observed with the same variation in the AEM Mg/Sb and V/Sb peak intensity ratios.

Thus the physicochemical characterization does not detect any change after the test in the case of the MgV(3/2)

system either in the noncalcined and calcined mechanical mixtures or in the impregnated samples.

The case of the mixtures containing MgV(2/2) seems very different. The formation of a new phase, $MgSb_2O_6$, was already detected by X-ray diffraction measurements when the MMgV(2/2)IVSb mixture was calcined at 823 K for 24 h. A sample color change was also observed. No new phase could be detected by XRD in the noncalcined MMgV(2/2)ISb(ia) after the test. Calcination of MMgV(2/2)ISb(ia) during the test (12 h) is not sufficient to produce crystallized $MgSb_2O_6$ (see Section 2.2.1.e). However, XPS results indicate that similar changes take place in both noncalcined MMgV(2/2)ISb(ia) during the test and in calcined MMgV(2/2)IVSb/*T* catalysts. The decrease in the XPS V/Sb atomic ratios in MMgV(2/2)ISb(ia) after the test (see Table 5A) and the similar XPS V/Sb atomic ratios observed in both noncalcined MMgV(2/2)ISb(ia) after the test and in calcined MMgV(2/2)IVSb/*T* (see Table 8A) seem to be due to the formation of a new phase, containing more antimony than vanadium, at the surface; this would be traces of $MgSb_2O_6$.

In such a reaction where an element (Mg) is both in the starting material (MgV(2/2)) and in a surface product ($MgSb_2O_6$) it is difficult to predict the changes in the corresponding XPS signal. The changes after test or after calcination are indeed relatively small (Table 5A) or even undetectable (Table 8A). This remark also holds for the impregnated MgV(2/2)III/*L* samples (see Table 7B), which will be discussed below.

We notice that the XPS Sb/(V + Mg + Sb) atomic ratios are not altered by test or by calcination. This is what could be expected if Sb on the surface of α-Sb_2O_4 would be used to form $MgSb_2O_6$. This confirms that $MgSb_2O_6$ is mainly located on the surface of the mixed sample. As the morphology of both solid reactants (MgV(2/2) and α-Sb_2O_4) changes during a solid-state transformation, it is difficult to go further in the interpretation and to indicate whether $MgSb_2O_6$ is preferentially on the surface of MgV(2/2) or α-Sb_2O_4.

The formation of $MgSb_2O_6$ in the mixtures of MgV(2/2) and α-Sb_2O_4 does not bring about measurable changes of BET surface areas. This is logical if $MgSb_2O_6$ covers MgV(2/2) as suggested by the XPS results.

The situation is different in the impregnated samples. Antimony in that case is initially very highly dispersed as shown by the high XPS Sb/(V + Mg + Sb) atomic ratios.

The decrease in the XPS Sb/(V + Mg + Sb) atomic ratio after the test indicates that the highly dispersed Sb_xO_y species formed on MgV(2/2)III or MgV(3/2)III sinters and detaches partially from the MgV(*X*)III surface.

The similarity of the XPS Sb/(V + Mg + Sb) atomic ratio before and after the test for the MgV(2/2)III/1 catalyst may be due to the fact that the Sb precursor is not completely decomposed or due to a small sintering of Sb at surface. However, it is not excluded that the stability in the XPS atomic ratio could also be interpreted by the balance of two simultaneous phenomena, on the one hand the decomposition of the precursor (or sintering) and on the other the contamination of the surface of MgV(2/2)III. These results show that if contamination is produced it is very limited. The principal phenomenon when the amount of Sb increases is the sintering of the antimony oxide crystallites on the surface of MgV(2/2)III.

A large number of tiny α-Sb_2O_4 crystallites would thus form. This would lead to an increase in BET surface area, as observed in other cases (38). This is indeed what we observed.

As a general conclusion of this section, catalysts containing MgV(3/2) are composed of two separate phases in contact. For those containing MgV(2/2), $MgSb_2O_6$ is present in small quantities in addition to the magnesium vanadate and α-Sb_2O_4.

4.3. Interpretation of the Catalytic Activity Results

At this point, a comparison of the catalytic results in terms of selectivity to propene is possible, taking into account that (i) the selectivity is approximately constant, when varying the amount of the single-phase catalysts, over a conversion range of 8% width (see Fig. 5) and (ii) for the MMgV(3/2)Sb and MMgV(2/2)Sb systems, conversion levels are approximately constant for $Rm = 0.25, 0.50$, and 0.75 (see Tables 12A and 12B) (in the range selected for the single-phase catalysts, MgV(*X*) ($X = 1/2, 2/2, 3/2$), however, the selectivities are quite different for both types of catalysts). A similar behavior is observed in the MMgV(3/2)0MgV(2/2) system.

This fact cannot be explained by considering the different amounts of MgV(2/2) or MgV(3/2) in the mixtures. Thus, another phenomenon might be considered to explain the trends of the catalytic results showed by those systems.

The nonlinearity of the conversion with the mass of catalyst is explained by the inhibitory role of reaction products. Propene, water, CO, and CO_2 very likely compete with propane for the catalytic sites. As the amount of active phase increases, more reaction products are present in the gas phase, and the inhibition increases, thus diminishing the contribution of additional quantities of catalysts.

The assumption that above 10% of conversion level, side reactions would not be completely avoided is another point to take into account for the interpretation of the synergetic effects. Synergetic effects must be put into evidence at low conversion to facilitate the possible explanations. This is the case of the MMgV(3/2)Sb(ia) system for which high selectivities are observed for conversion levels below 10%.

4.3.1. MgV(3/2)Sb System

The above discussion shows that the catalytic activity of mechanical mixture of MgV(3/2) and α-Sb_2O_4 must be

explained by a cooperative mechanism involving two separate, noncontaminated phases.

We are thus led to the conclusion that some cooperation via a mobile surface species takes place.

As in most of the reactions involving oxygen, α-Sb_2O_4 is not active but it is known as a donor of mobile oxygen species (21–22). The role of α-Sb_2O_4 in the present system would also be to produce mobile oxygen species which would migrate to the surface of MgV(3/2). This would be responsible for the modification of the catalytic performance.

Mobile oxygen species can play two roles: (i) react with propane adsorbed on MgV(3/2) (spill-over oxygen used as a reactant) and (ii) migrate to the surface of MgV(3/2) and react with it to modify the properties of the catalytic sites and improve the selectivity (spill-over oxygen used as a control species).

In the first case, the principal role of α-Sb_2O_4 would be to increase propane conversion. Our results show similar or slightly lower conversion, compared to those observed in the absence of the synergetic effect. We therefore come to the conclusion that the role of spill-over oxygen is to modify the catalytic sites.

The active MgV(3/2) would contain not only the catalytic sites for the OD of propane but also, in large proportion, those for the total oxidation. Spill-over oxygen would modify the sites responsible for total oxidation. This explains why the addition of antimony while maintaining propene yield, diminishes the overall formation of CO_2 (and, consequently, propene conversion).

This explanation is valid both for the mixtures and the impregnated catalysts. In impregnated MgV(3/2)III/*L*, a detachment of α-Sb_2O_4 during the reaction is observed. The tiny α-Sb_2O_4 crystallites thus formed play the same role as α-Sb_2O_4 admixed with MgV(3/2).

4.3.2. MgV(2/2) Sb System

The real structure of the catalysts containing MgV(2/2) is complicated due to $MgSb_2O_6$ formation on the surface during catalytic test. This formation may take place only during the test, before the new phase can be detected by X-ray diffraction. $MgSb_2O_6$ is a surface species and may cover either MgV(2/2) or α-Sb_2O_4 or both. Not surprisingly, the catalytic tests show complicated trends.

We tested separately prepared $MgSb_2O_6$. This phase produces only CO_2. When $MgSb_2O_6$ is mixed with α-Sb_2O_4, a significant increase in oxidation of propane to CO_2 and H_2O is observed. The dramatic increase in CO_2 production when MgV(2/2) has been impregnated with a high amount of Sb and calcined confirms the conclusion that $MgSb_2O_6$ catalyzes complete oxidation of propane.

The catalyst impregnated with one monolayer of Sb ions is less active than the nonimpregnated one. This can be explained by the fact that at low temperatures (773 K) the precursor is not completely decomposed and it blocks part of the sites on MgV(2/2). With increased temperature (813 K), the conversion is just similar to the nonimpregnated catalyst; this probably arises from the sintering of impregnated Sb ions. Interestingly the selectivity is higher in MgV(2/2)III/1 compared to the nonimpregnated catalyst. Conversely, when the Sb loading increases (MgV(2/2)III/3), conversion and yield increases but selectivity decreases.

The essential conclusion is thus that the synergetic effects in conversion are eventually due to the formation of $MgSb_2O_6$. It is not clear whether a cooperative effect between MgV(2/2) and α-Sb_2O_4 takes place in addition.

4.3.3. MgV(2/2)MgV(3/2) System

The cooperation between MgV(2/2) and MgV(3/2) has to be explained, as for MgV(3/2) + α-Sb_2O_4, by the contact between two uncontaminated phases.

For the same reasons as in the latter case, this cooperation has to be explained by a remote control mechanism. It is striking that we had to accept this explanation also in the case of mixtures of VPO catalysts (19, 20).

The existence of a cooperation between MgV(2/2) and MgV(3/2) gives arguments to explain the differences observed in the literature concerning the role of the activity and selectivity of the pyro and the ortho phases. The respective roles of MgV(2/2) and MgV(3/2) in the donor–acceptor pair constituting the actors in the remote control mechanism must be identified.

MgV(2/2)II shows both high propane conversion and CO_2 production, which increase as a function of temperature. In contrast, MgV(3/2)II shows both low propane conversion and CO_2 production, which remain nearly constant with temperature.

As a whole, mixtures with $Rm = 0.5$ exhibit a gain in conversion of propane and in propene yield and selectivity and a diminution in CO_2 formation.

But it seems difficult to analyze the effects in more detail. The addition of MgV(3/2) to MgV(2/2), to make the mixture of composition $Rm = 0.25$, brings relatively small effects. One could just conclude that MgV(3/2) is not a very efficient donor, and, perhaps, that it produces nonselective electrophilic species as shown by the increase in CO_2 production. This is not incompatible with the fact that α-Sb_2O_4 improves its selectivity. The conclusion would be that MgV(3/2) possesses a mixed function as both donor (but of electrophilic oxygen) and acceptor. If we now take as the majority phase this same MgV(3/2) and add 25% of MgV(2/2) (mixture of $Rm = 0.75$) some synergy appears and slightly less CO_2 is produced. MgV(2/2) thus appears as a donor of selective oxygen species (nucleophilic).

A confirmation of this conclusion could in principle be obtained by mixing MgV(2/2) with a donor: if MgV(2/2)

is a donor, another donor would have no promoting effect on it. Unfortunately, α-Sb_2O_4, which has no catalytic activity of its own, produces a compound of very low selectivity, namely $MgSb_2O_6$, when contacted with MgV(2/2).

Our conclusion must therefore be restricted to the fact that there is a synergy for conversion, and to a certain extent propene yield, between MgV(2/2) and MgV(3/2). It seems very likely that both phases have a dual role, donor and acceptor (especially MgV(3/2)), but it is not clear whether one of these role's is predominant.

Concerning MgV(1/2), it seems that a deterioration in selectivity is observed when MgV(2/2) or MgV(3/2) is mixed with it. The cooperation effects between phases by the remote control mechanism implies an increase in the selectivity; for this reason this mechanism does not operate when MgV(1/2) is present.

A tentative explanation of the deterioration in the selectivity can be related to the nature of the oxygen species present in the MgV(1/2) catalysts. These species are able to attack the hydrocarbon molecules and break its bonds, form radicals, and facilitate the formation of nonselective products. The fact that MgV(1/2) is active and nonselective is in line with this explanation. However, further studies are necessary to make a further evaluation of these catalysts.

4.4. Thermoreduction and Acidity

The ease in which MgV(2/2)0 is reduced compared to MgV(3/2)0 (see Fig. 4) has been correlated with the higher selectivity exhibited by pyrovanadate catalysts (8, 9). This higher selectivity had been attributed to the particular structure of the pyrovanadate phase (7–9). This consists of rows of V_2O_7 units, in which two sharing distorted tetrahedra are bridged by long V–O bonds. The selectivity-determining step of the reaction was supposed to be the one involving this bridging oxygen (7–9).

However, our results show that this could be the case only at low propane conversion. At high propane conversion, a decrease in propene selectivity is observed for MgV(2/2) catalysts (see Table 11), the selectivity being even lower than that of MgV(3/2) catalysts.

A correlation between relative weight change and selectivity indicates different trends in MMgV(2/2)0Sb and MMgV(3/2)0Sb catalysts. Whereas MMgV(2/2)0Sb shows higher relative weight change (see Fig. 4B) compared to MgV(2/2)0 (see Fig. 4A) and no synergetic effects regarding selectivity, the higher relative weight change observed in MMgV(3/2)0Sb compared to that of MgV(3/2)0 is correlated with synergetic effects regarding selectivity. This indicates that the correlation between reduction rate and selectivity is more complicated. It therefore seems that the explanation cannot be exclusively the different local environment of vanadium by oxygen atoms in the pyro- and orthovanadate structures.

Regarding the correlation between acidic properties and selectivity in the case of MgV(3/2)0Sb mixtures, a decrease in the acid site numbers compared to those of pure MgV(3/2)0 could be associated with the increase in selectivity exhibited by these catalysts. This effect is in contrast to that observed in the VPO catalyst in which the high selectivity observed in the presence of α-Sb_2O_4 during the oxidation of butane to maleic anhydride was correlated with high acidity. Thus, it could be suggested that a lower acidity is necessary to improve OD of propane. However, to prove this assumption studies in much more detail related to acidity strength and distribution of the acid sites are necessary. We remark that in the present study the distribution of the acid sites has been arbitrary assigned.

5. CONCLUSIONS

1. Synergetic effects are observed in the OD of propane in MgV(3/2) and MgV(2/2) oxides when they are in presence of α-Sb_2O_4 (mechanical mixtures and impregnated catalysts).

In the MgV(3/2)Sb system the principal effect is an increase in the selectivity with a corresponding decrease in propane conversion. In the MgV(2/2)Sb system the principal effect is a strong increase in propane conversion with a moderate increase in propene yield.

2. Physicochemical characterization showed that no formation of a new phase or contamination in the presence of α-Sb_2O_4 takes place when MgV(3/2) is used.

In the MgV(2/2)Sb system, a new phase, $MgSb_2O_6$, is formed during the catalytic test.

3. The remote control mechanism seems to be the most plausible explanation for the synergetic effects observed in catalysts containing MgV(3/2) and α-Sb_2O_4. The role of spill-over oxygen produced by α-Sb_2O_4 (Donor) would be that of inhibiting the nonselective sites. The same mechanism explains the synergetic effects found in the mixtures of MgV(3/2) and MgV(2/2). Both phases probably have a dual role, donor and acceptor.

The interpretation of the synergetic effects observed in the MgV(2/2) system is more complicated due to the presence of the new phase, $MgSb_2O_6$. It seems that $MgSb_2O_6$ is responsible for the high increase in propane conversion; that increase corresponds mainly to complete oxidation.

ACKNOWLEDGMENTS

The support of the Région Wallonne (Belgium) in the frame of an "Action Concertée" is greatfully acknowledged. Financial support from DGICYT (Programa FPU), Ministerio de Educación y Ciencia de España is greatfully acknowledged by S. R. G. Carrazán.

REFERENCES

1. Chaar, M. A., Patel, D., Kung, M. C., and Kung, H. H., *J. Catal.* **105,** 483 (1987).

2. Chaar, M. A., Patel, D., Kung, M. C., and Kung, H. H., *J. Catal.* **109,** 463 (1988).
3. Inomata, M., Miyamoto, A., and Murakami, Y., *J. Phys. Chem.* **85,** 2372 (1981).
4. Iwamoto, M., Takenaka, T., Matsukami, K., Hirata, J., Kagawa, S., and Izumi, J., *Appl. Catal.* **16,** 153 (1985).
5. Griffith, W. P., and Gonzales, F., *J. Chem. Soc., Dalton Trans.* 1416 (1972).
6. Moser, T. P., and Schrader, G. L., *J. Catal.* **92,** 216 (1985).
7. Siew Hew Sam, D., Soenen, V., and Volta, J. C., *J. Catal.* **123,** 417 (1990).
8. Guerrero Ruiz, A., Rodriguez Ramos, I., Fierro, J. L. G., Soenen, V., Hermann, J. M., and Volta, J. C., *in* ''Studies in Surface Science and Catalysis'' (V. Cortés and S. Vic, Eds.), Vol. 72, p. 203. Elsevier, Amsterdam, 1992.
9. Michalakos, P. M., Kung, M. C., Jahan, I., and Kung, H. H., *J. Catal.* **140,** 226 (1993).
10. Wang, R., Mimming, X., and Piug, L., *Catal. Lett.* **24,** 67 (1994).
11. Gao, X., Ruiz, P., Xin, Q., Guo, X., and Delmon, B., *Catal. Lett.* **23,** 321 (1994).
12. Gao, X., Ruiz, P., Xin, Q., Guo, X., and Delmon, B., *J. Catal.* **148,** 56 (1994).
13. Weng, L. T., Spitaels, N., Yasse, B., Ladriere, J., Ruiz, P., and Delmon B., *J. Catal.* **132,** 319 (1991).
14. Zhou, B., Sham, E., Machej, T., Bertrand, P., Ruiz, P., and Delmon, B., *J. Catal.* **132,** 157 (1991).
15. Weng, L. T., and Delmon, B., *Appl. Catal.* **81,** 141 (1992).
16. Cadus, L. E., Xiong, Y. L., Gotor, F. J., Acosta, D., Naud, J., Ruiz, P., and Delmon, B., *in* ''Studies in Surface Science and Catalysis'' (V. Cortés and S. Vic, Eds.), Vol. 82, p. 41. Elsevier, Amsterdam, 1994.
17. Castillo, R., Awasarkar, P. A., Papadopoulou, Ch., Acosta, D., and Ruiz, P., *in* ''Studies in Surface Science and Catalysis'' (V. Cortés and S. Vic, Eds.), Vol. 82, p. 795. Elsevier, Amsterdam, 1994.
18. Qiu, F. Y., Weng, L. T., Ruiz, P., and Delmon, B., *Appl. Catal.* **47,** 115 (1989).
19. Bastians, Ph., Genet, M., Daza, L., Acosta, D., Ruiz, P., and Delmon, B., *in* ''Third European Workshop Meeting on Selective Oxidation by Heterogeneous Catalysis.'' Louvain la Neuve, 1991.
20. Ruiz, P., Bastians, Ph., Cassin, L., Reuze, R., Daza, L., Acosta, D., and Delmon, B., *Catal. Today* **16,** 99 (1993).
21. Weng L. T., Duprez, D., Ruiz, P., and Delmon, B., *J. Mol. Catal.* **52,** 349 (1989).
22. Mestl, G., Ruiz, P., Delmon, B., and Knözinger, H., *J. Phys. Chem.* **98,** 11283 (1994).
23. Courthy, Ph., Ajot, H., Marcilly, Ch., and Delmon, B., *Powder Technol.* **7,** 21 (1973).
24. Weng, L. T., Ruiz, P., and Delmon, B., *in* ''2nd. International Conference of Spill-over.'' Leipzig, 1989.
25. Ruiz, P., Bastians, Ph., Causin, L., Reuse, R., Daza, L., Acosta, D., and Delmon, B., *Catal. Today* **16,** 99 (1993).
26. (a) Hoornaerts, S., Vande-Putte, D., Thyrion, F., Ruiz, P., and Delmon, B., *in* ''EUROPACAT-II'' Congress, The Netherlands, 1995; (b) Ruiz, P., Hoornaerts, S., Vande-Putte, D., Thyrion, F., and Delmon, B., submitted for publication; (c) Hoornaerts, S., Vande-Putte, D., Thyrion, F., Ruiz, P., and Delmon, B., *in* ''210th American Chemical Society National Meeting & Exposition Program; Division of Colloid & Surface Chemistry, Catalysis and Photocatalysis on Metal Oxides.'' Chicago, Illinois, 1995.
27. Haber, J., *Pure Appl. Chem.* **63,** 1227 (1991).
28. Galy and Pouchard, *Bull. Soc. Chim. Fr.* (ASTM file 23-1233) (1967).
29. Parker, F., and Cauley, Mc., private communication, ASTM file 34-13.
30. Clark, G., and Morley, R. J., *J. Solid State Chem.* **16,** 429 (1976).
31. Lubin, and Ritterhaus, private communication, ASTM file 10-779, 1966.
32. Nogier, J. P., and Delamar, M., *Catal. Today* **20,** 109 (1994).
33. Nogier, J. P., Jammul, N., and Delamar, M., *J. Electron, Spectrosc. Relat. Phenom.* **56,** 279 (1991).
34. Schuhl. Y., Baussart, H., Delobel, R., Le Bras, M., Leroy, J., Gengembre, L., and Grimblot, J., *J. Chem. Soc. Faraday Trans. I* **79,** 2055 (1983).
35. Nefedov, V. I., Firsov, M. N., and Shaplygin, I. S., *J. Electron Spectrosc. Relat. Phenom.* **26,** 65 (1982).
36. Colton, R. J., and Guzman, A. M., *J. Appl. Phys.* **49,** 409 (1978).
37. Horvarth, B., Strutz, J., Geyeer-Lippmann, J., and Horvarth, E. G., *Z. Anorg. Allg. Chem.* **483,** 181 (1981).
38. Xiong, Y., Weng, L. T., Bing, Z., Ruiz, P., and Delmon., *in* ''Studies in Surface Science and Catalysis'' (G. Poncelet, P. A. Jacobs, P. Grange, and B. Delmon, Eds.), Vol. 63, p. 537. Elsevier, Amsterdam, 1990.